UNIVERSITY OF CALGARY

Association of Kinesin Light Chain 3 with Outer Dense Fibers

by

Ying Zhang

A THESIS

SUBMITTED TO THE FACULTY OF GRADUATE STUDIES

IN PARTIAL FULFILMENT OF THE REQUIREMENTS FOR THE

DEGREE OF MASTER OF SCIENCE

DEPARTMENT OF

BIOCHEMISTRY AND MOLECULAR BIOLOGY

CALGARY, ALBERTA

JULY 2003

UNIVERSITY OF CALGARY

FACULTY OF GRADUATE STUDIES

The undersigned certify that they have read, and recommend to the Faculty of Graduate Studies for acceptance, a thesis entitled " Association of Kinesin Light Chain 3 with Outer Dense Fibers " submitted by Ying Zhang in partial fulfilment of the requirements of the degree of Master of Science.

Dr. Frans A. van der Hoorn, Department of Biochemistry & Molecular Biology

Dr. Patrick W.K. Lee, Department of Microbiology & Infectious Diseases

Dr. Derrick E. Rancourt, Department of Biochemistry & Molecular Biology

Dr. Jerome B. Rattner, Department of Biochemistry & Molecular Biology

Dr. Manfred J. Lohka, Department of Biological Sciences

Date Aug 29'03

Abstract

Conventional kinesin I motor molecules are heterotetramers consisting of two kinesin light chains (KLCs) and two kinesin heavy chains. The interaction between the heavy and light chains is mediated by the KLC heptad repeat (HR), a leucine zipper-like motif. Kinesins bind to microtubules and are involved in various cellular functions, including transport and cell division. Our lab recently isolated a novel KLC gene, klc3. klc3 is the only known KLC expressed in post-meiotic male germ cells. A monoclonal anti-KLC3 antibody was developed that, in immunoelectron microscopy, detects KLC3 protein associated with outer dense fibers (ODFs), unique structural components of sperm tails. No significant binding of KLC3 with microtubules was observed with this monoclonal antibody. In vitro experiments showed that KLC3-ODF binding occurred in the absence of kinesin heavy chains or microtubules and required the KLC3 HR. ODF1, a major ODF protein, was identified as the KLC3 binding partner. The ODF1 leucine zipper and the KLC3 HR mediated the interaction. These results identify and characterize a novel interaction between a KLC and a non-microtubule macromolecular structure and suggest that KLC3 could play a microtubule-independent role during formation of sperm tails.

Acknowledgements

I wish to extend sincere thanks to my supervisor, Dr. Frans van der Hoorn for his invaluable guidance and encouragement.

A special note of appreciation is extended to Dr. R. Oko in Queen's University for his electromicroscopy results and advice.

A special thank you to my supervisory committee, Dr. Petrick Lee, Dr. Derrick Rancourt and Dr. J.B. Rattner, for their critical advice.

A special thank you to the members of our laboratory, for all their friendship and help.

Finally, I would like to thank my wonderful family for their constant and never-ending love and support.

TABLE OF CONTENTS

LIST OF TABLES

LIST OF FIGURES

LIST OF ABBREVIATIONS

Ampr	ampicillin resistance
APP	amyloid precursor protein
ATP	adenosine 5'-triphosphate
bp	base pair
CGP	Cys- Gly-Pro repeat
CT	carboxyl terminal
EDTA	ethylenediamine tetraacetic acid
FS	fibrous sheath
g	gram
GST	glutathione S-transferase
His	histidine
HR	heptade repeats
hr	hour
JIP3	Jun amino-terminal kinase (JNK)-interacting protein 3
JNK	Jun amino-terminal kinase
KAP	Kinesin Associated Protein
kb	kilo base pair
kDa	kilo Dalton
KHC	Kinesin Heavy Chain
KIF	Kinesin Superfamily Protein
KLC	Kinesin Light Chain

KRP	Kinesin Related Protein
Leu	leucine
M	molar/L
mAb	monoclonal antibody
MBP	maltose-binding protein
mg	milligram
Min	minute
ml	milliliter
MT	microtubules
NP-40	Nonidet p-40
NT	amino terminal
OD	optical density
ODF	Outer Dense Fiber
pAb	polyclonal antibody
PAGE	polyacrylamide gel electrophoresis
pBS	pBluescript II (+) vector
PCR	polymerase chain reaction
PMSF	phenylmethylsulfonyl fluoride
RNAsin	ribonuclease inhibitor
SDS	sodium dodecyl sulfate
ST	seminiferous tubules
TBS	Tris-HCl-buffered saline
TE	Tris-EDTA buffer

TNT	transcription and coupled translation system
TPR	tandem tetratricopeptide repeat
Trp	tryptophan
μg	microgram
μl	microlitre
V	volume

CHAPTER I: INTRODUCTION

Spermatogenesis is characterized by continuous germ cell proliferation and differentiation. It takes place in seminiferous tubules, where developing germ cells undergo a series of characteristic differentiation steps in close association with somatic Sertoli cells. After an initial proliferatine phase, mitotically active spermatogonia enter a pre-meiotic phase and become spermatocytes. Upon completion of meiosis, haploid cells called spermatids, emerge. Spermatids differentiate into spermatozoa through a process known as spermiogenesis. The mammalian spermatozoa are free and motile cells, which are composed of two main parts, the head and the tail. Among the major morphological changes that occur at spermiogenesis is the formation of the sperm tail, which is composed of three major cytoskeletal elements, the axoneme, the out dense fiber (ODF), and the fibrous sheath (FS). These two latter elements are unique to spermatozoa, distinguishing the tail of the sperm from simple cilia and flagella. A distinct region of the tail is the midpiece, which contains all mitochondria surrounding the ODF and axoneme, but lacks the FS. Mitochondria migrate from the head during spermiogenesis. The ODF is composed of fibers, which surround and attach to the axoneme. Two ODF major proteins have been cloned from rat and mouse: Odf1 (27Kda) Odf2 (80Kda). Despite their probable important function in sperm integrity, motility, and durability, knowledge about the ODF formation as well as and its function is only rudimentary.

Conventional kinesin protein is a mechanochemical enzyme involved in plus-end directed translocation of membrane bound organelles on microtubules (MT). It consists two heavy chains (KHC) and two light chains (KLC). KHC has a tripartite structure based on functional domains. KHCs hydrolyze ATP and interact with microtubules at their globular, amino-terminal heads. Compared with KHC, less is known about the

functions of KLC. KLC are localized to the tail portion of KHCs, in close vicinity to the putative cargo-binding site. Based on its location within kinesin, KLC was predicted to mediate either cargo binding or regulation of kinesin. KLCs were originally cloned from rat, and subsequently homologues were isolated from numerous organisms. In mouse and rat, three KLC genes, KLC1, KLC2 and KLC3 had been identified. KLC1 plays a role in neuronal transport and KLC2 appears more widely expressed. KLC3 is a testis specific protein and accumulated in the sperm tail midpiece. In mouse and rat testis, KLC3 protein expression is restricted to elongating spermatids and KLC3 accumulates in sperm tails, in contrast to KLC1 and KLC2, which can only be detected before meiosis. The characterization of the KLC3 gene suggests that it carries out a unique and specialized role in elongating spermatids. The function of KLC3 in spermatogenesis remains a matter of investigation.

The purpose of this present study is to identify the function of KLC3, the 56kDa kinesin light chain protein, in spermatogenesis. My approach was to investigate the localization of KLC3 in spermatids, then explore the interactions between KLC3 and other testis specific proteins and further study its predicted cargo transport function.

CHAPTER II: LITERATURE REVIEW

2.1 Spermatogenesis and spermatozoa structure

Spermatogenesis

Spermatogenesis is characterized by continuous germ cell proliferation and differentiation. It occurs in the seminiferous tubules of the testis and can be divided into three intervals: (i) stem cell differentiation and renewal, (ii) meiosis, and (iii) spermiogenesis. The process of spermatogenesis begins with the stem cell, the spermatogonium, which is next to the basal lamina. The spermatogonium is a relatively small cell. Once sexual maturity is reached, the cell goes through a series of mitotic divisions. At this point during these divisions in the clone of the spermatogonia will divide both to differentiate and to renew the spermatogonium (Clermont, 1966). In rat, division leads to type A and B spermatogonia. The type B spermatogonium becomes a spermatocyte that will undergo meiosis (Dym, 1970).

During the first stage of meiosis the cells go through six recognizable stages based on the appearance and arrangement of chromosomes. The stages are: preleptotene, leptotene, zygotene, diplotene and diakinesis. Following this period of prophase the spermatocyte goes through two consecutive reduction divisions to form haploid spermatids (Clermont, 1966).

Spermiogenesis is the third and final stage of spermatogenesis, during which the spermatid goes through an elaborate process of cytodifferentiation, producing the mature spermatozoa (figure 1). Spermiogenesis is divided into four phases: the Golgi phase, the cap phase, the acrosomic phase, and the maturation phase. The hallmark events that occur

Figure 1. The stages of germ cell development in rat

A. Show here are the designations given to rat sperm cells with the shown morphologies, at various stages of development during spermiogenesis. The individual stages are explained in more detail in Dym, 1970, from which this figure is adapted.

B. A schematic representation of a cross section of the rat testis is shown, depicting the organization of cells in seminiferous tubule. Note the relative positions of spermatogonia, spermatocyte, spermatids and elongate spermatids.

A

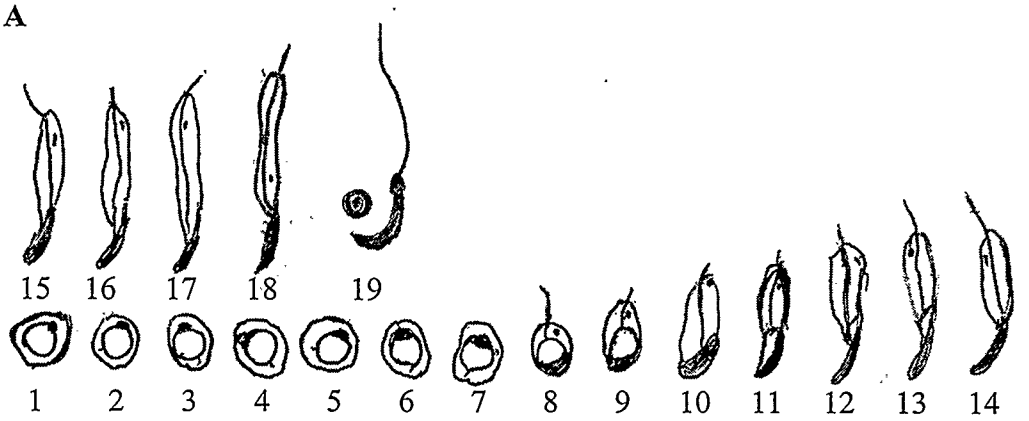
15 16 17 18 19
1 2 3 4 5 6 7 8 9 10 11 12 13 14

B

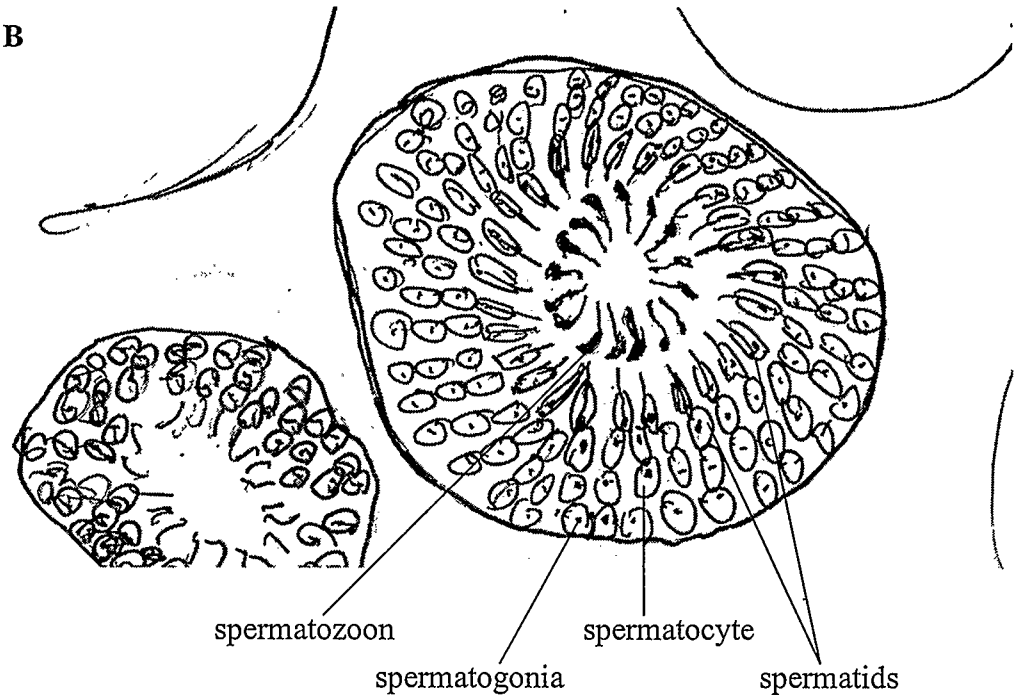
spermatozoon
spermatogonia
spermatocyte
spermatids

during the cap phase of spermiogenesis are the formation of the acrosomic granule and the migration of the centrioles to the cell plasms membrane opposite to where the acrosome is being formed. At the same time the assembly of the axoneme is being initiated. During the cap phase the acrosomic granule spreads over and covers the anterior half of the condensing nucleuses and elongates and the acrosomal cap conforms to the changing shape of the spermatid head. In addition the mitochondria begins to migrate to a region known as the middle piece of the sperm tail. The last phase in spermiogenesis is the maturation phase; the accessory components of the tail (i.e. ODF, and FS) are formed. At the end of this phase is the residual cytoplasm and organelles except the mitochondria in the middle piece are shed and engulfed by the Sertoli cells. The spermatozoa are then released into the lumen of the seminiferous tubule as free cells. In rat, spermiogenesis has been divided by morphological criteria into 19 steps (figure 1) (Dym, 1970)

Structure of spermatozoa

Despite the fact that transcription terminates during mid-spermiogenesis, many changes, including the assembly of a sperm tail, formation of an acrosome, and extensive remodelling and reshaping of the nucleus, occur during spermiogenesis. The resulting sperm shapes are species-specific (Russell, 1990). The mammalian spermatozoa are free and motile cells composed of heads and tails. The head is made up of a condensed haploid nucleus encapsulated by a thin and dense layer of cytoplasmic material called the perinuclear theca to which the membrane-delimited acrosome is tightly attached.

Among the major morphological changes that occur at spermiogenesis is the formation of the sperm tail. The prominent structural components of the sperm tail were

first described after the introduction of the electron microscope (Fawcett, 1975). The tails of mammalian spermatozoa vary considerably in length depending on the species (e.g., It is 190- um long in the rat and only 60-um long in man.). It consists of four main regions, namely the connecting piece, middle piece, principle piece, and end piece (figure 2) (Oko, 1990). The connecting piece is caudal to the sperm head. Its proximal component, houses the remnants of the proximal centriole, the capitulum, which is connected to the basal plate that lines the implantation fossa of the nucleus. Its distal component, the striated collar is connected to the outer dense fibers at the junctions of the connecting piece and middle piece. In the middle piece, along the axoneme, there are nine coarse outer dense fibers (ODF), each associated with one microtubular doublet (figure 2). Numerous condensed and elongated mitochondria are located along the middle piece, where they are helically and tightly disposed end to end around the outer dense fibers to form the mitochondrial sheath. The principal piece is characterized by the fibrous sheath (FS). It is composed of longitudinal columns and transverse ribs (figure 2). The longitudinal fibers replace ODF fibers 3 and 8 of the principal piece.

The axoneme composed of microtubules spans the entire length of the sperm tail. The major protein of the axoneme is tubulin, which is a dimer of α and β units. The axoneme has a 9+2 arrangement (figure 2) with dynein arms interactions between microtubules. The dynein molecules have ATPase and microtubular binding domains (Tang, 1981). The axoneme also has structures known as radial spokes that connects the two central singlets to the peripheral doublets of microtubules.

Figure 2. Diagram illustrating a rat spermatozoon with its sickle-shaped head and its 190 um-long tail

The four regions of the tail are indicated, i.e. the connecting piece (CP) joining the head and the tail, the middle piece (MP) showing the transversely oriented mitochondria, the principal piece (PP), and the end piece (EP). Electron micrograph gives the ultrastructure of the regions as seen in cross sections. This show the axoneme (microtubular doublets and singlets), the outer dense fibers, the fibrous sheath with the longitudinal columns and ribs, and mitochondria. The annulus is also shown at junction of the middle piece and principal piece. (Draw from Oko, 1990).

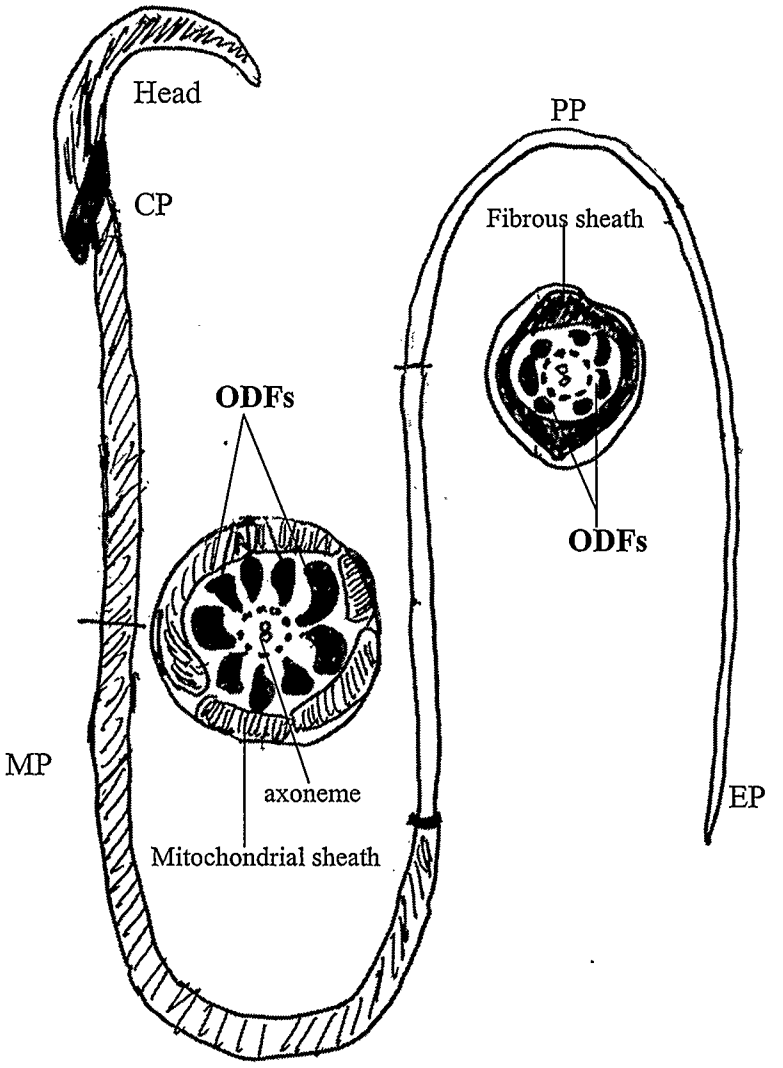
Head
CP
PP
Fibrous sheath
ODFs
ODFs
MP
axoneme
Mitochondrial sheath
EP

2.2 Outer Dense Fibers

Structure and Biogenesis

The ODF, together with the FS, are the unique cytoskeletal structures to spermatids. ODF is found in the middle piece and the principle piece of the sperm tail. Each fiber has its characteristic shape and is associated with an individual microtubular doublet of the axoneme giving a 9 + 2 arrangement around a pair of the microtubular singlets (figure 2). It is composed of a thin cortex surrounding a thick medulla (Fawcett, 1970). ODFs are common to all mammalian sperm and also found in the sperm of many other animal phyla, in particular those, which are characterized by internal fertilization (Baccetti, 1986).

The biogenesis of the outer dense fiber occurs in spermiogenesis. The precursor of the nine ODFs appears in step 8 of rat spermatogenesis (Irons, 1982). The rudimentary fibers form next to each of the microtubular doublet and are assemble in a proximal to distal direction along the tail. During step 15-16 of spermiogenesis a rapid and massive increase in diameter of the ODF occurs throughout its length (reviewed by Oko, 1990). In step 16 the entire length increases in thickness from the proximal to the distal aspect of the fibers. After step 16 the growth gradually decreases. Studies using autoradiography to localize metabolically incorporated proline and cysteine suggest that rapid protein synthesis accompany the growth of the ODF during step 16. This was confirmed by immunocytochemical studies done by Oko and Clermont (Oko, 1989).

Protein Composition

ODFs, as well as the FS, have the special property of being resistant to solubilization in ionic detergents because of their high content of disulfide bonds (Calvin, 1971). Earlier studies on the biochemical composition of ODFs have demonstrated that disulfide bond cross-linking of ODFs and FS proteins increased during epididymal transit and that zinc was a constituent of the ODFs proteins and probably involved in regulating the extent of disulfide cross-bridging (Calvin, 1979)

The outer dense fibers of mammalian sperm consist of several proteins in the molecular mass range from about 11kDa to about 110kDa (Olson, 1980; Vera, 1984; Oko; 1988; Henkel, 1992; Petersen, 2002). They seem to be the outer dense fiber specific. The protein composition of ODFs has been studied in several mammalian species. In humans, ODF consist of about 10 major and of at least 15 minor proteins (Hinkle, 1992; Petersen C 1999). In rat spermatozoa, the ODFs are composed of six major polypeptides (30-, 27-, 20-, 14-, 84- and 80kDa) (Vera, 1984) and of at least 14 polypeptides (Oko, 1988). Amino acid composition analysis showed that the major rat ODF polypeptides have high contents of lysine, arginine, cysteine, aspartate, serine, leucine and proline. In addition, these major polypeptides are found to be phosphorylated at serine resides (Vera 1984; Oko, 1988). The varying phosphorylation states of these polypeptides may provide some role in the regulation of flagellar motility.

The first cloned major ODF protein is Odf1, which was previously called RT7, Odf27, and rts5/1. Odf1 has a molecular mass of about 27kDa and a high cysteine and proline content. It is also the main zinc-binding protein of the sperm tail. The gene encoding this major ODF protein (odf1) has been isolated from rat (van der Hoorn, 1990;

Burfeind, 1991; Morales, 1994), human (Gastmann, 1993,) mouse (Hoyer-Fender, 1995), boar and bull (Kim, 1995). Their protein sequences display greater than 80% similarity. Rat Odf1 is very abundantly expressed as a 1.1kb mRNA in male germ cells, particularly, in early spermatids (van der Hoorn, 1990). Odf1 protein has two potentially functional domains: the N-terminal amphipathic ∝ helix, which is reminiscent of the leucine zipper dimerization protein motif (van der Hoorn 1990), and a C-terminal Cys-Gly-Pro (CGP) repeat (Higgy, 1994) that are found conserved in Drosophila Mst (3) proteins, which localize to Drosophila sperm tail fibers (Kuhn 1991; Schafer, 1993). A leucine zipper domain in the rat in part mediates self-interaction of Odf1. The C-terminal CGP repeats are involved in the interaction with OIP1, a putative E3 ligase RING zinc finger protein expressed in spermatids (Zarsky, 2003). Odf1 is sperm specific and localizes exclusively to the sperm tail in the ODF (van der Hoorn, 1990) and more specifically to the medulla of the ODF. Interestingly, by protein Blast search, two labs has recently reported that Odf1 clearly contains an alpha-crystallin domain that is characteristic for heat shock proteins, and classified it to be the 10th member of the superfamily of mammalian small stress proteins (Fontaine, 2003; Kappe, 2003). It is suggested that the ODF structural proteins may have other unknown functions.

Using Odf1 as bait in yeast two hybrid screens, two Odf1 interacting proteins have been cloned, Odf2 and Spag4, (Shao, 1997). Odf2 encodes an 84kDa protein and is another prominent protein of ODF. Odf2 was first cloned from rat by Shao (Shao, 1997) and Brohmann (Brohmann, 1997). Mouse odf2 was cloned and characterized by Hoyer-fender (Hoyer-Fender, 1998). In 1999, Peterson cloned human Odf2 that encodes a

70kDa protein. Sequence analysis showed that variability in sequence is restricted to specific regions in the N-terminal part of the encoded proteins, whereas the C-terminal part is highly conserved in Odf2 proteins between rat, mouse and human, pointing to a high evolutionary pressure residing on these proteins (Petersen, 1999). The conserved C-terminal region contains two leucine zipper motifs that are required for interaction with Odf1. Odf1 and Odf2 can interact with each other (Shao, 1997) and the Odf2 proteins have been shown to be heterogeneous (Brohmann, 1997). Unlike the medullar expression of Odf1, Odf2 localized to the connecting piece and both the cortex and medulla of the ODF. Cortical localization of Odf2 suggests that it may act as a structural link between the inner and outer regions of ODFs (Schalles, 1998). Recently, Nakagawa observed that exogenously expressed and endogenous Odf2 are concentrated at the centrosomes in a microtubule-independent manner in various types of cells at both light and electron microscopic levels (Nakagawa, 2001). These data suggest that Odf2 is a general component of the KI-insoluble centrosome scaffold, and not a sperm-specific protein: it is likely that in sperm tails Odf2 is specifically utilized to form the outer dense fibers.

Recently, several ODF associate proteins have been reported which belong to a group of chaperone-like ODF-binding molecular designated Spags, including spag4 (Shao, 1997) and Spag5 (Shao, 2001). Spags appear to drive ODFs to a precise destination (reviewed by Kierszenbaum, 2001a; Kierszenbaum, 2002b). Spag4 is an axoneme-binding protein, which strongly interacts with Odf1, the 27-kDa major ODF protein (Shao, 1999), via leucine zipper motifs. It is speculated to act as a link between ODFs and the axoneme. Spag5 has similarity to mitotic spindle protein and binds Odf1 also. It has two putative leucine zippers in the C-terminal part and the downstream one of

which is involved in interaction with Odf1. Together with the Odf1-Odf2 binding (Shao, 1997), these data suggested a crucial role for leucine zippers in molecular interactions during sperm tail morphogenesis.

Very recently, Petersen reported the isolation and molecular characterization of a novel gene of rat sperm ODF. They named it odf3. Odf3 is transcribed in testes and more specifically in spermatids but it is also expressed in epididymides and brain suggesting a possible involvement in building of the cellular cytoskeleton. Odf3 encodes a putative protein of approximately 110-kDa. Secondary structure predictions indicated that Odf3 is a coiled-coil protein (Petersen, 2002; Kierszenbaum, 2002b). The feature of Odf3 needs further investigation.

The function of ODFs remains unknown, but might be manifold, including strengthening of the long sperm tail, a function in elastic recoil; linking of the FS and mitochondrial sheath to the axoneme; and regulation of motility. It is expected that cloning and characterization of further ODF will aid in developing an understanding of the function of the structures.

2.3 Kinesin and Kinesin related proteins

The kinesin superfamily currently encompasses over 100 eukaryotic proteins containing a common motor domain. Both the nucleotide-binding fold and active-site chemistry of the motor domain are also present in the actin-based motor, myosin (Block, 1998). An excellent source of information is the kinesin home page (*www.proweb.org/kinesin/*).The kinesin superfamily proteins (KIFs) are mostly plus-end-

directed microtubule (MT) motors, although a few family members power minus-end directed transport (Amos, 1997). They are involved in the transport of organelles, protein complexes, and mRNAs to specific destinations (Hirokawa, 1996; Hirokawa1998; Brendza, 2000, Verhey, 2001) and also participate in chromosomal and spindle movements during mitosis and meiosis (Hirokawa, 1998; Sharp, 2000; Wild, 2001). Kinesins can be classified into three groups based on the position of their motor domains: N-terminal, C-terminal and internal kinesins (reviewed by Kull, 2000, Miki, 2001). Among numerous members of the kinesin superfamily, conventional kinesin (called kinesin-I, referred to throughout as kinesin) is a plus end directed microtubule based molecular motor (Vale, 1985a; Vale, 1985b). It was first found in squid axoplasm and was the first identified member of the kinesin superfamily. It is a mechanochemical enzyme, which powers the cytoplasmic transport of organelles and vesicles (MBOs) on microtubules (reviewed by Goldstein, 2001a; Kamal, 2002). MTs in cytoplasmic extensions including axons, dendrites and axonemes serve as polarized tracks for vectorial intracellular transport driven by MT-based motor proteins (Signor, 2000, Diez, 2002).

Native kinesin is a heterotetramer (figure 3) composed of two heavy chains (KHC) subunits (110-130kD) and two light chains (KLC) subunits (60-70kDa) (Bloom; 1988; Johnson, 1990; Kuznetsov, 1988). KHC has a tripartite structure (Yang, 1989) consisting of distinct domains with defined functions. At the N-terminus is a globular head, which hydrolyzes ATP, binds microtubules and is responsible for translocation on microtubules (Bloom, 1988; Hirokawa, 1989). The middle to C-terminal segment of KHC consists of an alpha-helical, coiled-coil rod-lick region, which medicates

Figure 3. Domain structure of conventional kinesin

Kinesin Heavy chain (KHC) contains the catalytic motor domain, the neck linker and neck domains, the coil1 and coil regions of the stalk domain, and the coiled and globular regions of the tail domain. Kinesin light chain (KLC) contains an ∝–helical heptad repeat region and six tetratricopeptide repeat (TPR) motifs (It is five in KLC3).

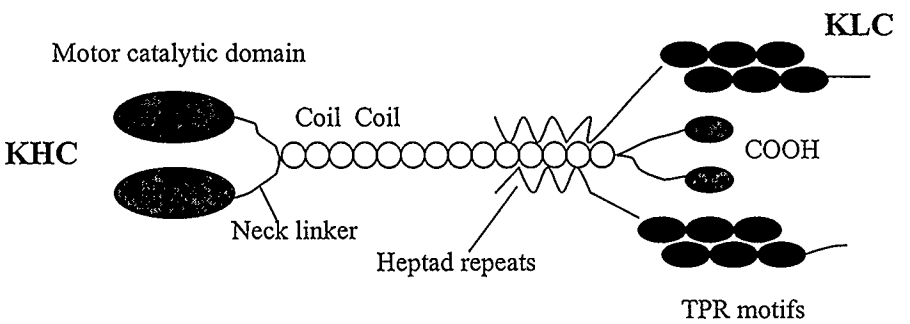
KLC
Motor catalytic domain
Coil Coil
KHC
COOH
Neck linker
Heptad repeats
TPR motifs

dimerization (de Cuevas, 1992). The extreme C-terminus of KHC consists of a small globular domain, which is the site of KLC and putative cargo attachment (Hirokawa, 1989; Hackney 1996) (figure 3). KLC subunits are probably involved in cargo binding or modulation of KHC activity (Bloom, 1995; Goldstein, 1999; Rahman, 1999; Kamal, 2000). Although only one conventional KHC gene is found in many species, including *Drosophila melanogaster* and Caenorbabditis elegans, mammals have three KHC genes (Kif5A, Kif5B, and Kif5C). Kif5B appears to be ubiquitously expressed, although its expression level is known to vary exclusively in the tissues (Hollenbeck, 1989). KIF5A on the other hand is expressed exclusively in neurons tissues (Niclas, 1994), and its expression differs from that of KIF5B during neuronal development (Vignali, 1996; Vignali, 1997). Kif5C is also thought to be neuronally enriched. As with the KLC genes, the tissue specific expression pattern of the different KIF isoforms has been interpreted as signifying distinct or specialized roles for the various kinesins in these tissues (Elluru, 1995). The three KHC genes are not completely functional redundant but rather specialized for a particular function. In mice, Kif5B knockouts prove to be embryonic lethal (Tanaka, 1998), as in the case for mutants in the single KHC gene of *Drosophila* (Saxton, 1991). The functions of Kif5A and Kif5C are unclear so far, although KIF5C has been suggested to be important for the viability of motor neurons (Kanai, 2000), and KIF5A mutations have been found to cause a form of hereditary spastic paraplegia in human (Reid, 2002).

Subsequent to the cloning of KHC, a large and ever expanding family of Kinesin Related Proteins (KRP) has been identified (Nakagawa, 1997). The family is characterized by a highly conserved motor domain for microtubule-based transport. Like

kinesin, the KRPs are thought to mediate transport of MBOs, and additionally have been implicated as key motors in mitotic, meiotic chromosome, spindle dynamics, the control of microtubule dynamics, transport of soluble protein components on recyclable "rafts", RNA movements, and potentially in functions not involving MT based motility. Unlike kinesin, the KRPs do not have associated light chains, although they do associate with various (often unidentified) Kinesin Associated Proteins (KAPs). For reviews see (Hirokawa, 1998; Goldstein, 1999; Marszalek, 2000; Gelfand, 2001). Kinesin and KRPs appear to be expressed in virtually all eukaryotes. Their widespread expression suggests that they play an essential role in cell physiology.

2.4 Kinesin Light Chain

Kinesin light chain (KLC) is another component of conventional kinesin. The first KLCs were cloned from rat brain and shown to exist as splice variants (KLCa, KLCb and KLCc) (Cyr, 1991). Subsequently, homologues of the rat KLC were cloned from *C. elegans* (Fan, 1994), sea urchin (Wedaman, 1993), squid (Beushausen, 1993), *Drosophila* (Gindhart, 1998, Gauger, 1993), and other mammals (Verhey, 1998; Khodjakov, 1998; Stenoien, 1997; Cabeza-Arvelaiz, 1993; Cyr, 1991). In addition to existing as splice variants, KLCs are also a multi-gene family including KLC1, KLC2, and KLC3. (Lamerdin, 1996; Rahman, 1998, Junco, 2001). In mouse, KLC1 is mostly neuronal and KLC2 is ubiquitous (Rahman, 1998). KLC3 was recently cloned from rat testis. Although KLC3 is also expressed in other tissues, including brain (Junco, 2001) and photoreceptors (Yang, 2002), spermatids are the major site of KLC3 expression (Junco, 2001) and KLC1 and KLC2 are not detectable in spermatids. The difference tissue expression patterns of

KLCs suggest unique needs for specific KLC gene products in particular tissues. Recent papers have predicted the KLCs' structure and putative function; however, the precise function of KLCs still needs further investigation.

The structure of KLCs

Analysis of KLC sequences revealed several conserved motifs in KLC family members as well as regions of divergence. The sequences at the N- and C-termini are highly variable, whereas the middle region contains highly conserved heptad repeats (HRs) and tandem tetratricopeptide repeats (TPRs) (figure 3).

KLCs share an N-terminal heptad repeat (HR), reminiscent of a leucine zipper motif. The HR region is predicted to fold as a coiled-coil, and is thought to mediate binding to KHC (Diefenbach, 1998; Gauger, 1993).

The middle region is highly conserved and consists of six tandem tetratricopeptide repeats (TPR) (Gindhart, 1996). KLC3 lacks the sixth TPR domain, which makes it to be the shortest KLC family member (Junco, 2001). Interestingly, the individual repeats of the TPRs are more highly conserved among species than individual repeats from the same organism. TPRs are predicted to form amphipathic helices, and in other proteins are known to mediate protein interactions. Their role in KLC function may be similar. Actually, it has been shown to mediate binding of kinesin to membrane bound vesicles (Stenoien, 1997).

The KLC also harbours a putative PEST motif, which is involved in protein degradation, between the HR and TPR. It has low sequence conservation, but with a large percentage of amino acids represented by proline, serine, threonine and aspartate

(Beushausen, 1993). The highly variable C-terminal region on KLCs has been proposed to bind cargo such as organelles and macromolecules (Khodjakov, 1998; Gyoeva, 2000).

KLC and Cargo transportation

Conventional kinesin is the most important one of the molecular motors that transports vesicle cargoes along microtubule tracks. It is relatively well understood how kinesin uses the energy of ATP to move towards the plus end of microtubules (reviewed by Signor, 2000; Thomas, 2002; and Howard, 2003) By contrast, our understanding of the cell biology mechanism of cargo transporting lags far behind. We do not even know the membranous cargo each kinesin carries, although some have been suggested (Goldstein, 1999; Goldstein, 2000). We do not know whether the motor connects directly to the cargo, and it is unclear how the motor picks up cargo at one site of the cell and releases it at its destination. The following review focus on the recently reports on these questions.

Based on its location within kinesin, KLC was predicted to mediate either cargo binding or regulation of kinesin (Hollenbeck, 1993; Hirokawa, 1989). KLCs localize to the c-terminus of the kinesin (figure 3), which lies outside the N-terminal motor domain (Hirokawa, 1989). This end of the tetramer is not required for the translation of kinesin along microtubules (Kuznetsov, 1989; Yang, 1990), and was therefore widely proposed to play a role in either binding cargo or regulating motor function, or both. Except the C-terminal subcellular localization, KLC antibodies studies and cell immunofluorescence study also suggest the KLCs contribute to cargo binding. An anti-KLC antibody inhibited binding of purified kinesin to isolated brain vesicles *in vitro* (Yu, 1992; Stenoien, 1997).

Drosophila KLC mutant experiments also support such a role of KLC: Large aggregates ("organelle jams") accumulate in axons, resulting from a block in axonal transport (Gindhart, 1998). KLCs have been reported to mediate the interaction between microtubules, kinesin, and membrane surfaces, including vesicles (Stenoien, 1997), microsomes (Yu, 1992), mitochondria (Khodjakov, 1998), and the trans-Golgi network (Gyoeva, 2000).

So far, two regions in kinesin light chain have been proposed for interaction with cargo: the conserved TPR motif and various C termini. Khodjakov stated that rat KLC1b binds via its C terminus to mitochondria in cultured CV1 cells and human skin fibroblasts (Khodjakov, 1998). Another KLC is co-purified with the Golgi membranes in western blot analysis and colocalizes with Golgi complex in cell. These data suggested that different splice variants of KLC may specifically target kinesin to distinct molecular cargoes (Gyoeva, 2000).

Although the function of the TPR domain of KLC was unknown, the TPR domain is thought to be involved in protein-protein interactions, and was thus postulated to link KLC to receptor proteins on vesicular or organelle cargoes. This suggestion has been confirmed by several studies. Stenoien and Brady reported that antibodies targeted to the TPR domain of KLC displace kinesin from membrane-bound vesicles without affecting ATPase activity of the motor or its ability to interact with microtubules (Stenoien, 1997). Recently, the study on the kinesin membrane receptors further confirmed that the TPR domain of KLC is involved in the cargo binding (Bowman, 2000; Kamal, 2000). A potential kinesin receptor, amyloid precursor protein (APP), which is a well-known transmembrane protein and related to Alzheimer's disease (Selkoe, 1999), has been found

to interact with the TPR domain of KLC (Kamal, 2000). In addition, the association of APP with microtubules and the axonal transport of APP are greatly decreased in a gene-targeted mouse-associated mutant lacking the gene encoding the neuronally enriched KLC1. Another kinesin binding protein is the Sunday driver protein (syd), which was found in a genetic screen for axonal transport mutants in *Drosophila.* Like APP, syd also binds to the TPR domain of KLC (Bowman, 2000). Sequence analysis of syd found that it is identical to a Jun amino-terminal kinase (JNK)-interacting protein 3(JIP3), a scaffolding protein for component of JNK signalling pathways (Ito, 1999). This result reveals a potential connection between signalling and vesicular transport by motor proteins (reviewed by Goldstein, 2001a).

Collectively, these results provide strong evidence for the KLC3 cargo binding. However, whether it is the kinesin heavy chain or the kinesin light chain subunit that binds to cargo has been questioned by some reports. Early in 1994, Skoufias has suggested that KHC along can bind membranes (Skoufias, 1994). In the Ascomycete fungus, *Neurospora crassa*, kinesin light chains are lacking (Steinberg, 1995). This also indicates that at least in these organisms, KHCs alone are sufficient by themselves for binding to some cargoes. It is likely that KHC coiled tail provides the binding site for cargo in these organisms (Seiler, 2000). Kinectin, an integral membrane protein localized to the endoplasmic reticulum, is the first reported potential receptor for kinesin (Toyoshima, 1992). Recently, it was fond to bind with kinesin heavy chain subunits (KIF5A, KIF5B, and KIF5C) in yeast two-hybrid and direct *in vitro* binding assays (Ong, 2000). One explanation is that both KLC and KHC can mediated the cargo binding, but in different cell type or for different cargoes. Further studies are needed to test it.

Another possible function of KLC is that it may regulate KHC and keep it in an inactive state by preventing the active conformation of KHC (Verhey, 1998). For example, an N-terminal 45kDa fragment of the kinesin tetramer and the KHC dimmer along both exhibit elevated MT stimulated ATPase activity (Hackney, 1991). Both of these molecules lack light chains. A mechanism is suggested by observations that the kinesin dimmer has a flexible hinge in the rod-like central domain (Amos, 1987). Additional evidence comes from KLC1 knockout mice: mutant mice were small and exhibited motor disabilities (Rahman, 1999). Also, in these mice, a pool of KHC KIF5A was mislocalized to the peripheral cis-Golgi.

2.5 Kinesins in testis

Successful spermatogenesis requires the participation of two principal cell types within the seminiferous epithelium: the gametogenic cells and supporting Sertoli cells. Each of these cell types contains an abundant and complex microtubule cytoskeleton that undergoes extensive rearrangement during the cycle of a spermatogenesis. The microtubule network of a spermatogenic cell reorganizes during its lifetime to form the mitotic and meiotic spindles, the spermatid manchette, and the sperm flagella. These suggest that testis should express a large number of MT motors for its various MT structures. However the characterization of kinesin and KRPs in this tissue remains minimal. Early evidence for the importance of MT transport in the testis comes from the observation that testis is an excellent source of cytoplasmic dynein (Collins, 1989; Neely, 1988).

On the other hand, the manchette, the sperm flagella and the Sertoli MT network offer more unique challenges for motor characterization. Immunolocalization and biochemical fractionation experiments have localized Kif5b heavy chains to the trans Golgi network in sertoli cells (Johnson, 1996; Hall, 1995), and the manchette in spermatids (Hall, 1992). Immunolocalization to the Golgi is consistent with a role for KHC in Golgi trafficking (Goldstein, 1999). Localization to the manchette raises the possibility that this MT network is involved in vesicular trafficking: in line with this, vesicles have been visualized in association with manchette microtubules (Rattner, 1972), However, the function of the manchette is not known, and thus Kif5b may fulfill a different function here. RT-PCR experiments suggested that in rat testis Kif5a is predominantly expressed in somatic testicular cells, but not expressed after meiosis. Kif5c is expressed at an extremely low level in spermatids but is not detectable in sperm tails (Junco. 2001). KifC5a has also been localized to the manchette (Navolanic, 2000).

KLC3 is recently cloned from rat testis, which contains a conserved HR motif that mediates binding to KHC, as well as 5 tetratrico peptide repeats (TPR) (Junco, 2001). In association with KHC, KLC3 binds to microtubules in an ATP-dependent manner. Analysis of different male germ cells demonstrated that spermatids are the major cell type for KLC3 expression and the protein accumulated in the midpiece of the sperm tail. Interestingly, male haploid germ cells do not have detectable amounts of synthesized KLC1 and KLC2, as determined by RT PCR, suggesting that KLC3 probably carries out their function in transport and other motor based processes and/or that other spermatid KLCs remain to be identified. This is in agreement with the observation that male KLC1 knockout mice are fertile (Stock, 1999).

Kinesin II family members have also localized to the sperm tail in the rat (Miller, 1999) and sea urchin/sand dollar (Henson, 1997). They consist of two different KIF3 motor proteins linked to the dynactin component (Karcher, 2002; Deacon, 2003). In the midpiece, the staining is similar to centrosomal staining. The staining was not detergent extractable, indicating that the kinesin II was not membrane associated, and further note+d a punctuate or discontinuous staining pattern with their antibody. Kinesin II has been implicated in the transport of intra flagellar transport particles (known as rafts) in *Chlamydomonas* (Cole, 1998). These rafts differ from MBOs, and may circulate as carriers of flagellar structural constituents such as inner dynein arms (Piperno, 1997). The paradigm may well be true for flagellar structures in higher eukaryotic organisms. It is important to note that.

Kinesin related proteins (KRP), which do not contain light chains, have also been described in rat testis (Sperry, 1996, Zou, 2002), two of which have sequence similarity to the previously described BimC subfamily of KRPs involved in mitosis (Kashina, 1997). The other KRPs expressed in the testis had no homology to known kinesins and likely represent novel family members. The KIF3 KRPs were also detected in testis: KIF3A and KIF3B form heterodimers that function as MT-based plus end transporters of membranous organelles (Yamazaki, 1995). A KIF3C knockout mouse is viable and apparently normal (Yang, 2001). Since kinesins and KRP transport cargo on MT tracks it is interesting that rat testicular KRP2 and KRP6 are associated with spindle MTs (Sperry, 1996). KRP3, a novel kinesin- related protein expressed in the mammalian testis was identified recently. At least two KRP3 isoforms are in the rat, KRP3A, KRP3B. KRP3 isoforms localize with the nuclei of developing spermatids, and their immuno localization

in the testis is overlaps with that of the small GTPase Ran. Like Ran, KPR3 motors are associated in a polarized fashion with the nucleus of maturing spermatids at various stages of elongation (Zou, 2002)

Together these data suggest that conventional kinesin as well as KRPs play a role in spermatid flagellar transport and the testis provide an excellent opportunity to study kinesins.

CHAPTER III: OBJECTIVES

KLC3 is a novel member of the kinesin light chain family. It possesses all of the characteristics of a genuine KLC. It contains a conserved HR motif that mediates binding to KHCs as well as five tetratricopeptide repeats. In association with KHC, KLC3 binds to microtubules in an ATP-dependent manner. KLC3 is expressed in several tissues, including testis and brain; analysis of different male germ cells demonstrated that spermatids are the major site of KLC3 expression. In mouse and rat testis, KLC3 protein expression is restricted to round and elongating spermatids, and KLC3 is present in sperm tails. In contrast, KLC1 and KLC2 can only be detected before meiosis in testis. Interestingly, the expression profiles of the three known KHCs and KLC3 differ significantly: Kif5a and Kif5b are not expressed after meiosis, and Kif5c is expressed at an extremely low level in spermatids but is not detectable in sperm tails. The characterization of the kinesin genes suggests that KLC3 carries out a unique and specialized role in spermatids

The question of KLC3's function in spermatids remains to be addressed and is closely linked to its interaction with other molecules. Based on our data, several possibilities present themselves. One is that an unknown KHC interacts with KLC3 in sperm tails. Alternatively, KLC3 may associate with another member of the extended kinesin-like family. We consider these two possibilities to be less likely, because genomic localization experiments show only three KHC genes in the mouse and no precedent exists for KLC interaction with any kinesin-like proteins other than KHC. However, related KHC genes of lower similarity would have been missed in the first assay. A third possibility is that the spermatid provides a unique environment in which the majority of KLC3 does not interact with a known KHC but with other sperm specific proteins.

The objectives of the present study are to investigate the localization of KLC3, the novel kinesin light chain, in developing spermatids, to explore the interactions between KLC3 and other testis specific proteins, and further study the possible molecular mechanisms for the interactions.

The study will contribute to understanding the possible functional roles of KLC3 in spermiogenesis.

CHAPTER IV: MATERIALS AND METHODS

4.1 Antibody Production

A fusion protein containing maltose-binding protein (MBP) linked to KLC3 was produced by inducing transfected TB1 bacteria with isopropyl-β-D-thiogalactopyranoside. Bacteria were lysed by sonication. After centrifugation, the MBP-KLC3 fusion protein was purified from the bacterial extract using amylose-agarose columns and eluted using maltose according to manufacture's instruction (New England Biolabs Inc.). Eluted fusion protein was analyzed by SDS-PAGE. For MAb production, 6-week-old BALB/c mice were injected with 10 μg of MBP-KLC3 fusion protein. For hybridoma production, SP2/MIL-6 myeloma cells (grown in Dulbecco's modified Eagle's medium supplemented with 10% fetal calf serum) were fused to spleen cells. MAb production was analyzed by immunofluorescence using frozen rat testicular sections and Western blot assays using NitroPlus membranes (Micron Separations Inc., Westboro, MA) onto which MBP-KLC3 had been transferred. Polyclonal antibodies were produced as follows. New Zealand White rabbits were injected with purified MBP-KLC3, initially with complete Freund's adjuvant and subsequent injections with incomplete Freund's adjuvant. Serum was collected and tested for KLC3 recognition by Western blot analysis as described above. Affinity-purified polyclonal anti-KLC3 antibody was isolated by incubation of total antibodies with membrane-immobilized MBP-KLC3 protein, washing of membrane strips, and elution of bound antibodies.

4.2 Plasmid Constructions

DNA fragments were obtained by restriction enzyme digestion of other plasmids containing the fragments of interest or by using the polymerase chain reaction (PCR). All

manipulations including subsequent ligation, competent cell preparation, transformation and plasmid DNA isolation were done using standard techniques as described by Sambrook (Sambrook, 2001). The *E. coli* XL-1 Blue (Stratagene) strain was used for all plasmid transformation. The orientation of the inserts was analyzed by appropriate restriction enzyme digestion or by sequencing. All the plasmid constructs are summarized in Table 1 in which their inserts and uses are indicated.

Plasmid construction for in vitro binding assay

Wild type KLC3 and KLC3ΔHR mutant-containing plasmids were obtained from our lab stock (Junco, 2001). They were cloned into the *EcoR*I and *Sal*I sites of pBluescript Ks (+) plasmid (figure 4A) in frame. The KLC3 C-terminal deletion (KLC3Δ C) was created by PCR using forward primer C1478 (5'-CGCTAAGTGGACTGGCTGCAG-3'), reverse primer C1174 (5'-GCTGAGGATCTCCTTGTATAGCTCC-3'), and pBS- (ATG) KLC3 (our lab stock) as a template. The pBSKHC and p21Ras are from our lab's previous work.

Plasmid construction for Yeast Two Hybrid Assay and GST fusion proteins

Wild-type KLC3 and mutants fragment were obtained through digestion of pBS plasmid constructs and cloned into *EcoR*I and *Sal*I of pGAD424 in frame. The vector was shown in Figure 4C. PGBT9-Odf1 mutants were made as described previously (Shao, 1997). Figure 4B shows the MCS of pGBT9. PGEX-KG Plasmids constructions for GST fusion protein expression were obtained from previous work in our lab (Shao, 1999).

Table 1. Plasmid constructs

plasmid	insert	use
pBS-KLC3	KLC3	In vitro translation
pBS-KLC3 Δ HR	KLC3 Δ HR	
pBS-KLC3 ΔC	KLC3 ΔC	
pBS-KHC	KHC	
RAS	RAS	
pGAD-KLC3 ΔC	KLC3 ΔC	Yeast Two-hybrid Assay
pGAD-KLC3 Δ HR	KLC3 Δ HR	
pGAD-KLC3NT	KLC3NT	
pGAD-KLC3	KLC3	
pGBT-ODF1NT	ODF1NT	
pGBT-ODF1CT	ODF1CT	
pGBT-ODF1NT100	ODF1NT100	
pGBT-ODF2	ODF2	
PET-Odf1	Odf1	Expression of GST-fusion proteins
PET-Odf1NT	Odf1NT	
PET-Odf1Δ NT	Odf1Δ NT	
PET-Odf1NT25-147	Odf1NT25-147	
PET-Odf1CT	Odf1CT	
PET-Odf1Δ CT	Odf1Δ CT	

Figure 4. Multiple cloning sites of vectors used

The pBluescript II KS (+) is a 2961bp plasmid whose multiple cloning sites (A) flanked by T3 and T7 RNA promoters. Ampicillin-resistance gene is for antibiotic selection. The KLC3 and mutants used in the *in vitro* translation assay were inserted into *EcoR*I and *Sal*I site.

PGAD424 generates a hybrid protein that contains the sequences for the GAL4 activation domain (amino acids 768-881). PGAD 424 has unique restriction sites located in the MCS region (C) at the 3' end of the open reading frame for the activation domain sequence. It carries the *Leu2* nutritional maker that allow yeast autotrophs carrying pGBT9 to grow on limiting synthetic medium lacking Leucine. The KLC3 fragments used in yeast two hybrid assays were inserted into *EcoR*I and *Sal*I site.

PGBT9 generates a hybrid protein that contains the sequence of the GAL4 DNA-Binding domain (DNA-BD; amino acid 1-147). It carries the TRP1 nutritional maker that allows yeast-carrying pGBT9 to grow on limiting synthetic medium lacking Trp. In yeast two hybrid assays ODF1 and mutants were inserted into *BamH*I site (B).

The expression vector pGEX-KG uses a pBR322 origin of DNA replication. The ampicillin resistance gene allows for the selection of the presence of the vector. GST is the gene for glutathione S-transferase, which serves as a tag for purification of the fusion protein. The presence of the $lacI^q$ gene in the plasmid assures that the *tac* promoter will not be transcribed until induced by IPTG. To produce the GST fusion protein, ODF1 DNA fragments were inserted into *BamH*I site in frame (D)

A. MCS reading frame in pBluescript II Ks (+) vector

T7 ...CAG GAA TTC GAT ATC AAG CTT ATC GAT ACC GTC GAC CTC...T3
EcoR I *Sal* I

B. MCS reading frame in pGBT9 vector

GAL4 DNA binding domain
→
TCG CCG GAA TTC CCG GGG ATC CGT CGA CCT GCA GCC AAG CTA ATT
EcoR I *Sal* I

C. MCS reading frame in pGAD424 vector

GAL4 activation domain
→
ATC GAA TTC CCG GGG ATC CGT CGA CCT GCA GAG ATC TAT GAA
EcoR I *Sal* I

D. MCS reading frame in pGEX-KG vector

GST
→
CGT GGA TCC CCG GGA ATT TCC GGT GGT GGT GGT GGA ATT CTA.....
BamH I *EcoR* I
Sma I

4.3 Immunocytochemistry analysis of KLC3 expression in testis

Adult male Sprague-Dawley rats were anesthetized, and their testes and epididymides were fixed by retrograde perfusion through the abdominal aortas either with standard Bouin's fixative for histology or with 0.8% glutaraldehyde and 4% paraformaldehyde in 0.1 M phosphate-buffered saline containing 50 mM lysine (pH 7.4) for ultrastructure. After perfusion, the tissue designated for electron microscopy was razor-cut into 1-mm^2 blocks, immersed in the respective fixative for 1 h, washed extensively with buffer, and processed for Lowicryl embedding. The tissue designated for light microscopy was razor-cut into 3-4-cm^2 blocks, immersed in Bouin's fixative overnight, washed several times over 1 day with 70% ethanol, and processed for paraffin embedding.

Immunohistochemistry

After an extensive wash with 70% ethanol, the tissue blocks were dehydrated and embedded in paraffin by standard procedures. Five-μm sections were deparaffinized, hydrated through a graded series of ethanol concentrations, and immunostained as previously described (Oko, 1998) using monoclonal and affinity-purified polyclonal KLC3 antibodies.

Immunoelectron microscopy

Processing of tissues for Lowicryl K4M embedding followed a standard protocol used in our laboratory. Lowicryl-embedded ultra thin sections of testes and epididymides were mounted on 200-mesh Formvar-coated nickel grids, transferred, and floated tissue

side down on 10-20-μl drops of the following solutions: 10% goat serum in 20 mM Tris-HCl-buffered saline (TBS) (pH 7.4), 15 min; anti-KLC3 MAb diluted 1:10 in TBS, 1 h; TBS containing 0.1% Tween 20, 5 × 5 min; 10% goat serum in TBS, 15 min; colloidal gold (10 nm)-conjugated goat anti-mouse IgG diluted 1:20 in TBS, 45 min; TBS containing Tween 20, 3 × 5 min; and distilled H_2O, 2 × 5 min. The sections were then counterstained with uranyl acetate and lead citrate and examined by electron microscopy. Controls consisted of replacing the primary antibody (anti-KLC3) step with TBS or mAbs raised against other proteins that were diluted 1:10 in TBS.

4.4 ODF purification and western blot analysis

ODFs were isolated from rat epididymis spermatozoa as described by Oko (Oko, 1988) and Shao (Shao, 1997).

Collection and preparation of spermatozoa

Epididymides were obtained from Sprague-Dawley rats. The epididymides were minced in a few drops of 0.02 M of Tris-buffered saline (TBS), at a pH of 7.4, and then suspended in 15 ml of the same buffer at 20C. The suspension was then stirred and filtered through 150 um Nitex netting (Thompson, Montreal, Quebec). The filtrate was then centrifuged at 400x g for 10 min; all subsequent steps were carried out at 4C, except where otherwise stated, and 0.2 mM phenylmethylsulfonyl fluoride (PMSF) was added to buffers. The sperm pellet was washed twice in 15 ml of TBS, and after the last centrifugation, was resuspended in 5 ml of TBS.

Isolation of sperm tails

The suspension of spermatozoa was sonicated at 4 °C with a Bronwill Biosonik IV, VWR sonicator (Scientific, San Francisco, CA) set to 100% output, for 15-s burst at 30-s interval. This procedure guarantees 95% decapitation as verified by phase contrast microscopy. After sonication was completed, 10 ml of TBS was added to the suspension, which was then centrifuged at 600-x g for 10 min. The pellet was resuspended in TBS containing 80% sucrose and centrifuged at 280 000 x g for 1h in a 60 Ti angle rotor (Beckman Mississauga, ON). The centripetal pellet, containing mostly tails was resuspended with 20 mM TBS in 60% (w/v) sucrose, which was then layered over a sucrose step gradient composed of 9-ml fractions of 80%, 70%, and 65% (w/v) sucrose in 2 mM TBS, and spun in a Beckman centrifuge SW 28 swing bucket rotor at 100,000 x g for 70 min. The sperm tails were then removed from the 65-70% interface with a contamination rate of 1%. The tail fraction was pooled and diluted in 30 ml of TBS and was pelleted at 10,000 x g for 15 min.

Isolation of the ODF

The final tail pellet was suspended in 8 ml of 25 mM TBS, pH 7.4, 1% SDS, and 2% DTT and shaken at room temperature at various times (1-3 h). All other tail components but the ODF was solubilized during this isolation. Freed ODF was then separated on a discontinuous sucrose gradient and the pure ODF fraction was then collected at the 35-75% interface after being spun at 100,000x g for 15 min. Finally; the pellet was weighed and used for protein gel electrophoresis, and electron microscopy studies.

SDS Polyacrylamide Gel Electrophoresis

Isolated ODF fraction was solubilized and homogenized in 2% SDS loading buffer for 5 min. at 100°C and run on 10-20% discontinuous linear gradient polyacrylamide gels. Up to 100 ug of protein was used in each lane of the gel. Gels were stained with Coomassie Brilliant Blue dye.

Western Blotting analysis

Proteins were separated by electrophoresis on SDS-polyacrylamide gels and transferred to Hybond-P polyvinylidene difluoride membranes (Amersham, Inc.) in a solution of 25mM Na_2HPO_2, pH 6.5, which was carried out on a Hoefer Transphor Apparatus (Hoefer Scientific Instruments, San Francisco, Ca). Electrophoretic transfer of the proteins was carried out at a voltage setting of 115V for 1.5 h. After transfer of the proteins from the gels was completed, the gel were stained by Coomassie Brilliant Blue, while the membrane blots were stained with 0.2% Ponceau Red in 3%TCA, to determine the effectiveness of the transfer of the proteins from the gel to the membranes. The PVDF blots were blocked overnight in TBS with 5% milk power. Specific proteins on blots were analyzed by incubation with antisera to ODF1, β-tubulin (Sigma), KHC (Chemicon International, Inc.), and KLC3, followed by horseradish peroxidase-coupled secondary antibodies. Blots were developed using chemiluminescence (LumiGLO chemiluminescent substrate system; Kirkegaard & Perrie Laboratories, Inc., Gaithersburg, MD).

4.5 *In vitro* transcription/ translation

In vitro translations were done using the TNT® Coupled Reticulocyte Lysate System (Promega), a transcription and translation coupled system. Reactions were performed as suggested by the manufacturers. 1 μl of TNT reaction buffer, 1μl of TNT RNA polymerase (T7 for KLC3, KHC; sp6 for RAS) were added to a tube containing 12.5μl of TNT Rabbit Reticulocyte Lysate. Then 0.5 μl of 1mM amino acid mixture minus cysteine, 2 μl of [^{35}S] cysteine (approximately 15uCi), 1μl of 40u/μl RNAsin Ribonuclease Inhibitor and 1μg DNA template were added to the mixture, and nuclease-free water was added to bring the reaction volume to 25ul.

4.6 KLC3-ODF *in vitro* binding assay

To analyze the binding of KLC3 protein to purified ODFs, PBS-KLC3, RAS plasmids were first used in the in vitro transcription and coupled translation system (TNT) to produce ^{35}S-cysteine–labeled proteins KLC3 and ras. Then the *in vitro* translated proteins were incubated with purified ODFs in the presence of 0.1% Sarkosyl , 0.5% Sarkosyl, 1% Triton X-100, and 1% NP-40. After binding, ODFs were pelleted through a 35% sucrose cushion, washed and repelleted several times, and analyzed by SDS-PAGE. Optimization of the concentration is determined by compare the radioactive signal in autoradiography film. The optimize binding buffer is expected to give strong signal in KLC3 binding results but lowest signal in Ras binding results.

KLC3, KLC3ΔHR, KLC3Δzip, or KHC was transcribed *in vitro* and translated in the presence of ^{35}S-cysteine using the TNT reticulocyte transcription and translation

system Radiolabeled proteins were incubated with purified ODFs at 30 °C for 15 min. ODFs were pelleted at 30,000 rpm for 15 min at 22 °C. Supernatants were saved for SDS-PAGE analysis. Two subsequent washing/pelleting reactions were performed. Aliquots of both supernatants and pellets were boiled in SDS sample buffer and analyzed by electrophoresis on 10% SDS-polyacrylamide gels, and the gels were dried and exposed to Biomax film (Eastman Kodak Co.) for 2 days. P21Ras was used as a negative control.

4.7 Yeast Two-hybrid KLC3 Interaction Assay

Preparation of Yeast Competent Cell

The yeast host strains: SFY526, HF7c were used in this experiment. Table 2 shows the genotype and reporters for each yeast strain.

Cells were inoculated from a single colony (2-3 mm in diameter) into 20 ml YPD medium (20g/l Difco peptone, 10g/l Yeast Extract, pH 5.8, 2% dextrose) and incubated at 30°C with shaking (230 rpm) until OD600 was 1-2. Then an amount of this overnight culture (10-20 ml) was transferred to 300 ml YPD medium in one-liter flask to produce an OD600 of 0.2 and further incubated for 3h. The cells were centrifuged at 3000 rpm in a clinical centrifuge for 5 min at room temperature, washed with 50 ml sterile water and resuspended in 1.5 ml of 1X TE/LiAc solution (10 mM Tris-HCl, 1mM EDTA, 0.1 M lithium acetate, Ph 7.5) (Schiestl, 1989).

Transformation of plasmids into yeast strain

Approximately, 0.1μg of DNA, together with 100 μg of denatured salmon sperm carrier DNA (4mg/ml), and 100 μl of the yeast competent cells were added to a 1.5 ml

Table 2 Genotype of the yeast host strain

Strain	Genotype	Reporter	Transformation Markers
SFY526	*MATa, ura3-52, his 3-200 Ade 2-101, lys 2-801, trp 1-901 Leu 2-3, 112, canr, gal4-542, Gal80-538, URA3:: GAL1-lacZ*	*lacZ*	trp1, leu2
HF7c	*MATa, ura3-52, his3-200 Lys2-801. Ade2-101, trp1-901 Leu2-3, 112, gal4-542, Gal180-538, LYS2::GAL1-HIS3, URA3::GAL4 (17-mers)3-CYC1-lacZ*	*HIS3* *lacZ*	Trp1, leu2

microcentrifuge tube and mixed well. 0.6 ml sterile PEG/LiAc solution (40% PEG 4000, 10mM Tris-HCl, 1mM EDTA, 0.1 mM lithium acetate, pH7.5) was added to each tube m mixed and incubated at 30°C for 30 min with shaking (200 rpm). Then 70 ul DMSO were added (to 10% final concentration) and mixed gently. The cells were then heat shocked for 15 min in a 42°C water bath, chilled on ice and pelleted by centrifugation for 5 sec at 14,000 rpm in a microfuge and resuspended in 0.5 ml of TE buffer. 0.1ml of the transformation mixture was spread onto a 100-mm plate containing the appropriate SD selection medium. The plate was incubated at 30°C for 3 days (Schiestl, 1989).

His3 Reporter Gene assay

4 colonies were picked up from each yeast strain HF7c transformation plate. Then plate 0.1ml cell mixtures onto SD/Leu-Trp-His- plates with different 3-AT concentration (0, 12.5, 17.5, 25, 50 mM) respectively. Incubate the SD/Leu-Trp-His- plates at 30°C for 2-3 days and observe the cell growth. Cell growth up indicated the positive interactions between the two hybrid proteins.

Filter assay for β–Galactosidase

4 colonies were picked up from each SD/Leu-Trp- plate from yeast strain SFY526 transformation and streak onto a new SD/Leu-Trp- plate, which is the master plate. Incubate the plate at 30°C for 1-2 days. A filter (VWR grade 413) was presoaked in 1.8 ml Z buffer / X-gal solution (100 ml Z buffer: 1.61 g $NaHPO_47H2O$, 0.55g $NaH_2PO_4H_2O$, 0.075 g KCl, 0.0246g $MgSO_47H_2O$, 0.27 ml β–mercaptoethanol, 1.67 ml

20 mg/ml X-gal). Another filter was placed over the surface of the agar plate containing the transformant colonies and oriented by making holes through the filter into the agar if necessary. The filter was then lifted off the agar plate with a forceps and submerged into a pool of liquid nitrogen for 10 sec. The filter was removed from the liquid nitrogen and thawed at room temperature. Then the filter was placed, yeast side up, on another filter that was presoaked in Z buffer/X-gal solution. The filter was incubated at 30°C for several days. Blue color on the filter indicated the positive interactions between the two hybrid proteins.

4.7 Protein-protein association assay using GST-fusion proteins

Preparation of GST fusion proteins

GST (glutathione S-transferase) fusion proteins were prepared as described by Frangioni and Neel (Frangioni, 1993) with some modifications made by Shao (Shao, 1996). A single colony of XL-1 Blue (Stratagene) transformed with the plasmid of interest was grown overnight in 1ml LB containing 50 μg/ml Ampicillin at 37°C with shaking. The overnight culture was added to 9ml fresh LB containing Ampicillin and grown for about 2 h until OD600 was 0.6-0.8. Bacteria were induced with 0.2 mM IPTG for 4hr at 37°C. Bacteria were pelleted and washed once with 2ml ice-cold STE (10mM Tris-HCl, pH8.0, 150mM NaCl, 1mM EDTA) and resuspended in 1.35 ml STE containing 100μg/ml of lysozyme and incubated on ice for 15min. DTT was added to a final concentration of 5mM. After vortexing for 5 sec, cell were sonicated on ice for 2 min and centrifuged at full speed in a microfuge at 4°C. The supernatant was transferred

to a new Eppendorf tube. Triton X-100 was added to a final concentration of 1% from a 10% stock in STE. 20μl of bacteria lysate was mixed with 2XSDS loading buffer and heated at 90°C for 15 min before loading to the 10% SDS PAGE. After running, the gel was stained by Coomassie.

GST-fusion protein association with in vitro translated protein

Glutathione agarose beads were preincubated in binding buffer (20mM Tris-HCI, pH7.5, 150 mM NaCl, 1 mM EDTA, 20 mg/ml BSA, 0.5% NP-40) for 2 hr. Approximately 12 μl of in vitro translation mix containing ^{35}S-cysteine labeled PT7 protein and approximately 2.5 μg of desired GST fusion protein were added to 20 μl preincubated beads (50% v/v in fresh binding buffer), 50 μl fresh binding buffer was added and the tube was incubated at 4C for 1 h. Then beads were pelleted and washed 4 times with 0.5 ml wash buffer (20 mM Tris-HCl, pH7.5, 150 mM NaCl, 1mM EDTA, 20mg/ml BSA, 0.5% NP-40, 0.01% sarkosyl). The supernatant was aspirated and 20 μl of reducing SDS-PAGE sample buffer (60 mM Tris-HCl, pH6.8, 2% SDS, 10% glycerol, 10% β-mercaptoethanol, 0.025% bromophenol blue) were added to the beads and fully denatured by heating to 95°C for 3 min. The samples were then separated on SDS-PAGE gels (Sambrook, 2001). Gels were stained with Coomassie brilliant Blue (G-250), destained, dried on a BioRad vacuum gel dryer and exposed to X-ray film for several days. The amount of GST and GST fusion proteins bound to glutathione agarose beads can be determined on the Coomassie Blue stained gels.

CHAPTER V: RESULTS

5.1 Localization of KLC3 to ODF Surfaces

KLC3 is concentrated in the midpieces of elongated spermatids

Kinesin light chains (KLCs) are components of the conventional kinesin motor molecule, which is a heterotetramer of two KHCs and two KLCs. In the mouse, two KLC genes, *KLC1* and *KLC2*, had been identified (Lamerdin, 1996, Rahman, 1998). KLC1 plays a role in neuronal transport, and KLC2 appears to be more widely expressed. Our lab recently cloned and characterized a novel gene, *klc3*, which has the distinguishing structural and functional features of KLC proteins (Junco, 2001). It interacts *in vitro* with the KHC, the interaction is mediated by a conserved heptad repeat sequence, and it associates *in vitro* with microtubules. Interestingly, it is found that spermatids express only KLC3, not the other known light chains KLC1 and KLC2. This suggested that KLC3 might carry out roles specific to the process of spermiogenesis in addition to a general function in transport. To analyze KLC3 protein localization during rat spermiogenesis, our lab generated affinity-purified polyclonal anti-KLC3 antibodies as well as monoclonal anti-KLC3 antibodies (Junco, 2001), both of which specifically recognized the 58-kDa KLC3 protein. These antibodies were used in immunocytochemistry study of rat testis sections later.

The process of spermatogenesis begins at puberty and occurs continuously in the epithelium of seminiferous tubules (ST) in the testis. It is characterized by continuous germ cell proliferation and differentiation. Using KLC3 monoclonal antibody and purified polyclonal antibody, our lab investigated the KLC3 expression pattern during spermiogenesis by immunocytochemistry. Figure 5 shows the results of immunocytochemistry using affinity-purified polyclonal antibodies and illustrates that

Figure 5. KLC3 expressions during spermiogenesis- polyclonal immunocytochemistry

Rat testicular sections were prepared, and KLC3 was visualized using affinity-purified polyclonal anti-KLC3 antibodies. Sections were counterstained with methylene blue. The *Roman numerals* refer to the stage of the cycle of the rat seminiferous epithelium of individual cross-sections. Note that KLC3 localized to the cell body of round spermatids at early stages of spermiogenesis and to the forming sperm tail at later stages. *Arrows* indicate lightly stained tails, and *arrowheads* indicate prominently stained tails. *White arrows* indicate predominately cytoplasmic staining. In some stages, KLC3 was also expressed in Sertoli cells. *Scale bars* = 40 μm.

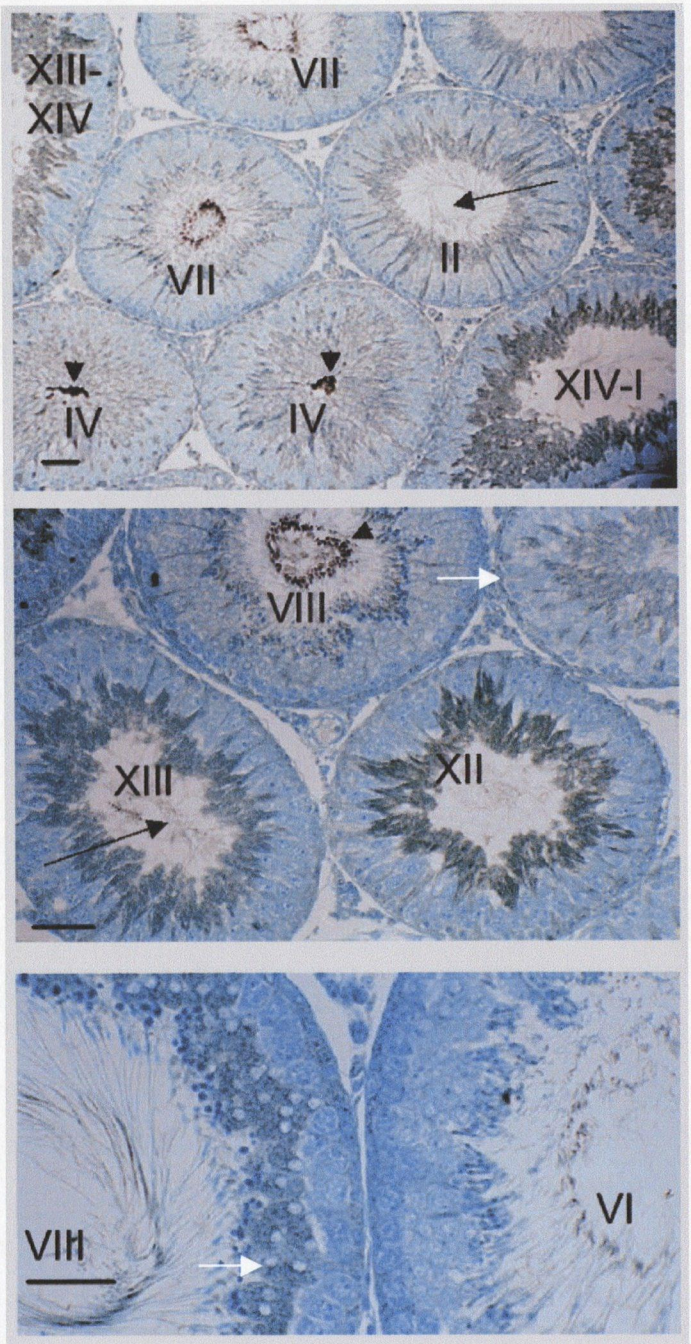
XIII-
XIV
VII
VII
II
IV
IV
XIV-I
VIII
XIII
XII
VIII
VI

KLC3 protein expression was first detectable in step 8 round spermatids (stage VIII of the seminiferous epithelium) (*middle* and *lower panels*). KLC3 immunostaining appeared to peak in the cytoplasm of elongating spermatids at stages XIV-I, thereafter gradually diminishing from this region (steps 16-19, stages II-VIII), but at the same time becoming prominent in the tails of maturing elongated spermatids. Initially, KLC3 staining in the tail was light (*arrows*), but later became very dense (*arrowheads*) along the entire tail. This suggests that KLC3 associates with structures that run the length of the tail, *viz.* the axoneme and/or ODFs. Figure 6 shows the results of immunocytochemical analyses using MAb B11. KLC3 labeling was first detectable in step 14 spermatids (figure 6*A*). Cytoplasmic staining became prominent from step 15 spermatids onwards and at later steps became concentrated in the midpiece area of elongated sperm tails (figure 6*B*). Figure 6*C* (and *inset*) shows cross-sections of midpieces, and figure 6*D* (and *inset*) shows longitudinal midpiece sections, both exposures revealing a strong KLC immunoreactivity in mature spermatids to be exfoliated. This result indicates that KLC3 proteins detected by the MAb are present in association with structures present in the sperm tail midpiece (*e.g.* the ODFs and/or mitochondrial sheath), but not the axoneme or FS. The results were summarized in figure 7. The *upper panel* summarizes the period of spermatid development showing KLC3 staining as detected by the polyclonal and monoclonal antibodies; the *lower panel* indicates schematically KLC3 staining in the cytoplasm and tail structures observed using the MAb.

The results of immunocytochemistry indicate that in late stage of spermiogenesis, KLC3 highly accumulated in sperm tail midpiece, a region containing the axoneme, ODF

Figure 6. KLC3 expressions during spermiogenesis- monoclonal immunocytochemistry

Rat testicular sections were analyzed as described in the legend to figure 5 except using anti-KLC3 mAb B11. Immunostaining was first observed in the cytoplasm of step 14 spermatids at stage XIV (*A*) and peaked in step 15-16 spermatids at stages I-III (*B*). KLC3 immunostaining could be observed in the midpieces of step 18-19 spermatids in cross-sections (*C*, *inset*) and in longitudinal sections (*D*, *inset*). *Scale bars* = 40 μm.

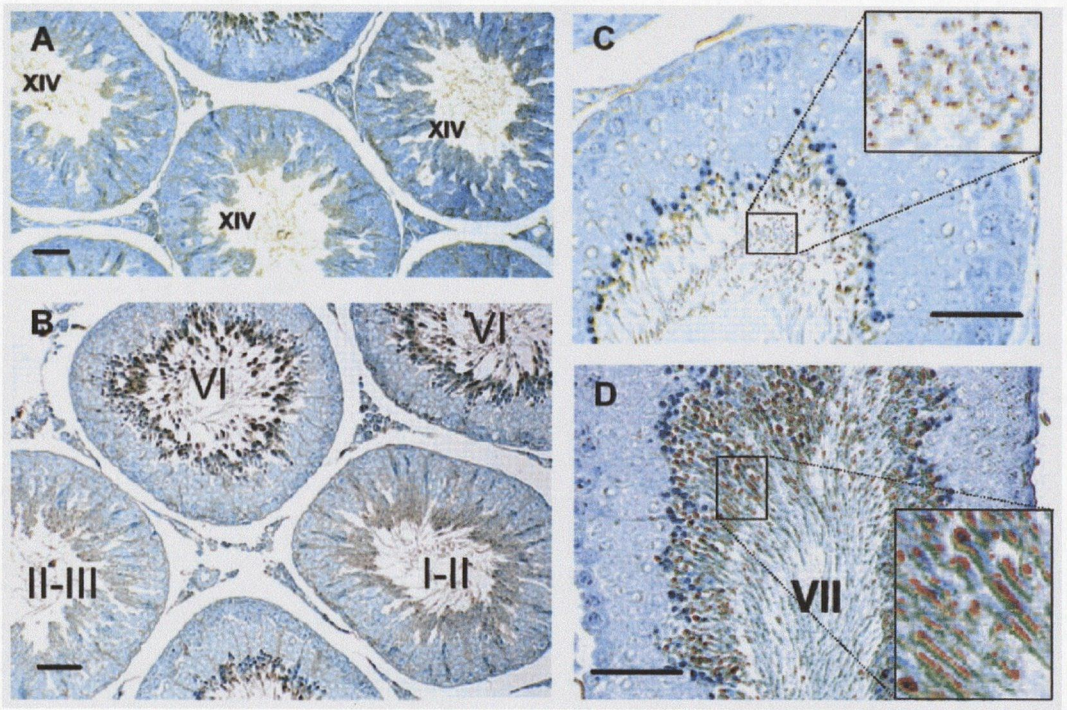
A
XIV
XIV
XIV
B
VI
VI
II-III
I-II
C
D
VII

Figure 7. Schematic drawing of the timing of KLC3 expression in sperm tails

Shown are schematic representations of timing (upper panel) and pattern of KLC3 expression (lower panel) in spermatids during spermiogenesis. Shown are spermatids at different developmental stages ranging from steps 1 to 19 (mature); levels and localization of KLC3 as detected by mAbs are indicated in shades of gray. KLC3 is first detected in step 12 spermatids. KLC3 protein accumulates in the midpiece at later stages. The midpiece (m) and head (h) are indicated.

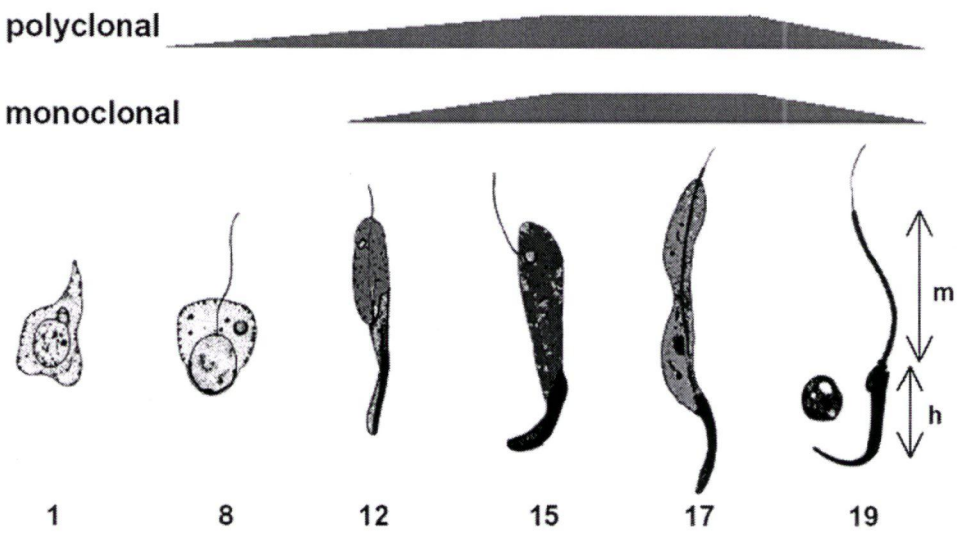
polyclonal
monoclonal
m
h
1
8
12
15
17
19

and the mitovhondrial sheath. KLC3 are not detectable at earlier stages of spermatogenesis (spermatogonial cells, spermatocytes or round spermatids).

Immunoelectron microscopy study shows KLC3 signal is around ODF

In the middle piece of mature sperm tail, along the axoneme, there are nine coarse outer dense fibers (ODF), each associated with one microtubular doublet (figure 2, Oko, 1990). Numerous condensed and elongated mitochondria are located along the middle piece, where they are helically and tightly disposed end to end around the outer dense fibers to form the mitochondrial sheath.

As described in figure 7, KLC3 immunoreactivity appeared concentrated in the midpieces of elongated spermatids. To further investigate the location of KLC3 in sperm tail midpiece. We used the KLC3 monoclonal antibodies in a more precise ultrastructural analysis. An adult rat epididymis was razor-cut into 1-mm^2 blocks and fixed for 1hour, and then processed for Lowicryl embedding as in Materials and Methods. Next, the sections were incubated with KLC3 MAb and colloidal gold-conjugated goat anti-mouse IgG separately. The sections were then counterstained with uranyl acetate and lead citrate and examined by electron microscopy. The results shown in figure 8 reveal a novel association pattern for KLC3 in mature step 19 elongated spermatids. Figure 8 (A and B) shows cross-sections, and figure 8C shows a longitudinal section through rat sperm. The MAb detected KLC3 predominantly in association with the surface of ODFs, but not with the axoneme, confirming the light microscopic observations with this antibody. The KLC3 immunogold label was also observed between adjacent ODFs and between ODFs and surrounding mitochondria (examples are shown in figure 8D). Quantitation of gold

Figure 8. Immunoelectron microscopic analysis of KLC3 distribution in sperm tails

Ultrastructural analysis of KLC3 localization in sperm tails was carried out using immunogold-labeled anti-KLC3 mAb B11. A and B, cross-sections through midpieces of mature sperm tails. Note that immunogold label was associated with the surface of ODFs. C, longitudinal section through the midpiece of a mature sperm tail. Label was often present between the mitochondrial sheath and the ODFs (arrows point to examples). smr, submitochondrial reticulum; ax, axoneme; odf, outer dense fibers; m, mitochondria. D, examples of gold label in association with ODFs. Scale bars = 0.1 μm. (From Dr. R. Oko)

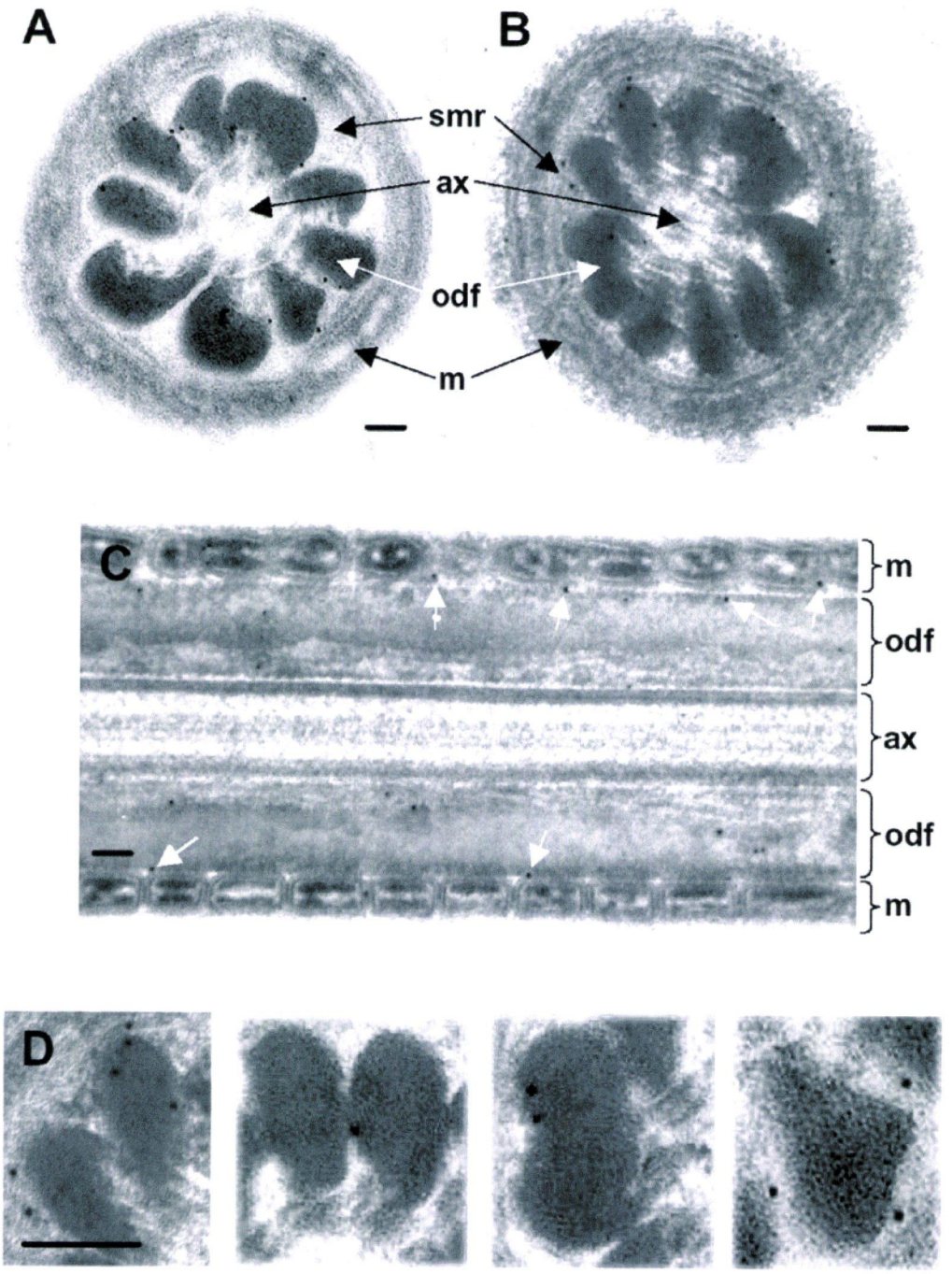
A
B
smr
ax
odf
m
C
m
odf
ax
odf
m
D

label in all micrographs indicated that labeling was not significant outside of this designated region, including sites within the ODFs, FS, or axoneme. In mature sperm, microtubules have not been shown to be present between adjacent ODFs or between mitochondria and ODFs (Hermo, 1991).

Based on these results, we conclude that MAb B11 detects KLC3 proteins that display a novel subcellular localization in elongating spermatids, and we proceeded to explore the possibility of a binding association of KLC3 with the macromolecular ODF structure.

5.2 The HR of KLC3 Is Involved in ODF Interaction

ODF isolation

The ODFs are cytoskeletal structures unique to spermatids. It is found in the middle piece and the principal piece of the sperm tail. Each fiber has its characteristic shape and is associated with an individual microtubular doublet of the axoneme giving 9+2 arrangement around a pair of microtubular singlets. The ODF is composed of a thin cortex surrounding a thick medulla. The protein composition of the outer dense fiber seems to be unique to the sperm (Irons, 1982; Oko, 1987; Shao, 1997; Shao, 2001).

To investigate the KLC3-ODF interaction *in vitro*, the ODFs were first isolated and purified from mature rat epididymal spermatozoa using gradient centrifugations as described in Materials and Methods. Phase microscopy was used during the whole process to check the changes of sperm tail structure. After the sperm tails were treated with SDS-DTT for 1h, the ODF was still attached to the connecting portion of the tail. At 1.5 h most of the connecting piece of the tail had been dissolved, freeing the ODF. The

ODF proteins then were isolated in 10-20% SDS-PAGE electrophoresis. The Coomassie blue stained gel revealed the polypeptide bands, of which the 84-, 80-, 27 (+30)-, 20-, and 14- kDa polypeptides were the most prominent (figure 9A) in rat ODF.

Purified ODFs do not contain KHC or β-tubulin

As described above, KLC3 shares some characteristics with KLC1 and KLC2. It interacts *in vitro* with the KHC and associates *in vitro* with microtubules in the presence of KHC and ATP. To make sure there is no interpretation in the following binding assay from the KHC and MT contamination, purified ODFs were examined by Western blot analysis to confirm that they were completely devoid of endogenous β-tubulin (MT) and KHC. I also tested them for the presence of KLC3 using KLC3 polyclonal antibody. Figure 9B shows that purified ODFs did not contain detectable β-tubulin or KHC, indicating that the ODF preparations were not contaminated with axonemal components. In addition, we did not detect KLC3 in purified ODF preparations, indicating that, as suggested by the immunoelectron microscopic data, KLC3 is an ODF-associated protein rather than an integral ODF protein and is lost in the ODF isolation procedures. Controls for all three proteins were positive. Brain expressed KHC; microtubule preparations contained β-tubulin; and testis expressed KLC3, as expected.

KLC3 can bind to isolated ODFs in vitro

An *in vitro* ODF binding assay was developed to study the molecular basis of the novel KLC3-ODF association observed in elongating spermatids. First, PBS-KLC3, p21-

Figure 9. Purified ODFs do not contain KHC or β-tubulin

A. Coomassie Brilliant blue stained 10-20% linear gradient SDS-polyacrylamide gel of the isolated rat outer dense fiber (ODF). Showed the primary ODF proteins Odf1 (27kDa), Odf2 (84kDa) and 14kDa protein P14. B To investigate the presence of KHC, β-tubulin, and KLC3 in purified ODF preparations, Western blot analysis was done comparing ODFs with the indicated positive controls. The antisera used in this analysis are indicated below the lanes and include anti-KHC (KHC), anti-β tubulin (tub), anti-KLC3 (KLC3), and, as positive control for ODF, anti-ODF2 (ODF2). odf, purified ODFs; brain, total brain extract; brain mt, purified brain microtubules; sperm, sperm tails. Note that ODFs contained ODF2 as expected, but not any of the other proteins analyzed.

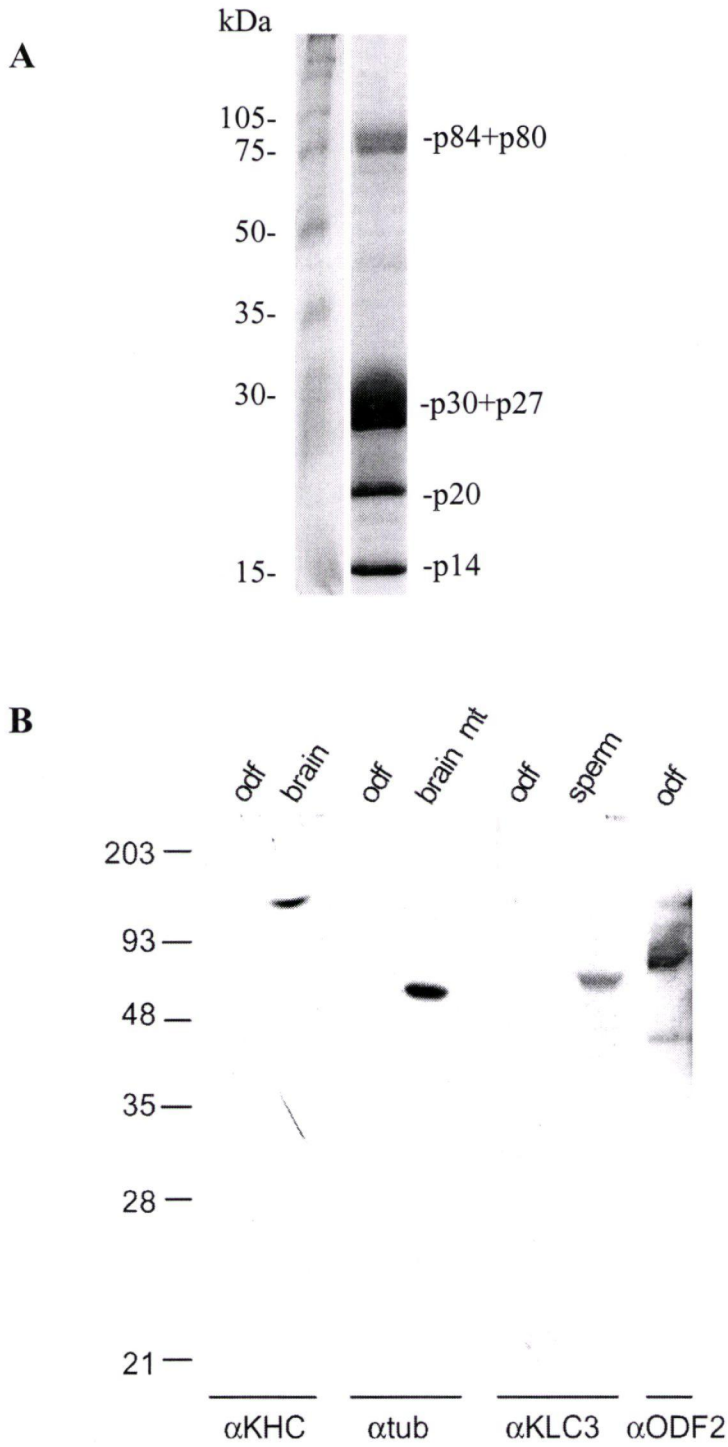
A
kDa
105-
75-
50-
35-
30-
15-
-p84+p80
-p30+p27
-p20
-p14
B
odf
brain
odf
brain mt
odf
sperm
odf
203
93
48
35
28
21
αKHC
αtub
αKLC3
αODF2

RAS plasmids were used in the in vitro transcription and coupled translation system (TNT) to produce ^{35}S-cysteine labeled proteins (Translations panels in figure 10)

Next, in vitro translated ^{35}S-radiolabeled KLC3 was added to purified ODFs in the presence of different concentration of detergents (0.1% Sarkosyl , 0.5% Sarkosyl, 1% Triton X-100 and 1% NP-40). Detergents were used here to get rid of non-specific interactions. An unrelated protein (p21ras) was used as a negative control (figure 10, low panel). After binding, ODFs were pelleted through a sucrose cushion, washed and repelleted several times, and analyzed by SDS-PAGE. The results show that wild-type KLC3 (58 kDa) could bind to purify ODFs in the presence of all kinds of detergents, but the Ras oncoprotein failed to bind in the presence of 0.1% and 0.5% sarkosyl. These results suggest that KLC3 can interact with ODFs strongly *in vitro*. In the later *in vitro* binding experiments, I used 0.1% sarkosyl in the binding buffer as a standard assay.

The HR of KLC3 Is Involved in ODF Interaction

KLC3 can be classified as a genuine light chain. It shares the same motif domain with other kinesin light chains. Its N-terminal has a heptad repeat (HR), reminiscent of a leucine zipper motif that is involved in binding to KHCs (Gauger, 1993; Verhey, 1998). The middle region is highly conserved and consists of tandem tetratricopeptide-repeats that, in other proteins, mediate protein interactions (Gindhart, 1999). The highly variable C-terminal region of KLCs has been proposed to bind cargoes such as organelles and macromolecules; this is supported by direct binding studies in which rat KLC1b was shown to bind to mitochondria (Khodjakov, 1998) and by the use of specific antibodies that bind to KLC and block its interaction with organelles (Stenoien, 1997).

Figure 10. *In vitro* translated KLC3 binds to purified ODF in the presence of 0.1% Sarkosyl

PBS-KLC3, RAS plasmids were used in the *in vitro* transcription and coupled translation system (TNT) to produce ^{35}S-cysteine–labeled proteins KLC3 and Ras. Ras was used as a nonspecific control for ODF binding here. Then the in vitro translated proteins were incubated with purified ODFs in the presence of 0.1% Sarkosyl , 0.5% Sarkosyl, 1% Triton X-100 and 1% NP-40. After binding, ODFs were pelleted through a sucrose cushion, washed and repelleted several times, and analyzed by SDS-PAGE. The results show that wild-type KLC3 (58 kDa) could bind to purified ODFs in the absence of 0.1% and 0.5% sarkosyl, but the Ras oncoprotein failed to bind.

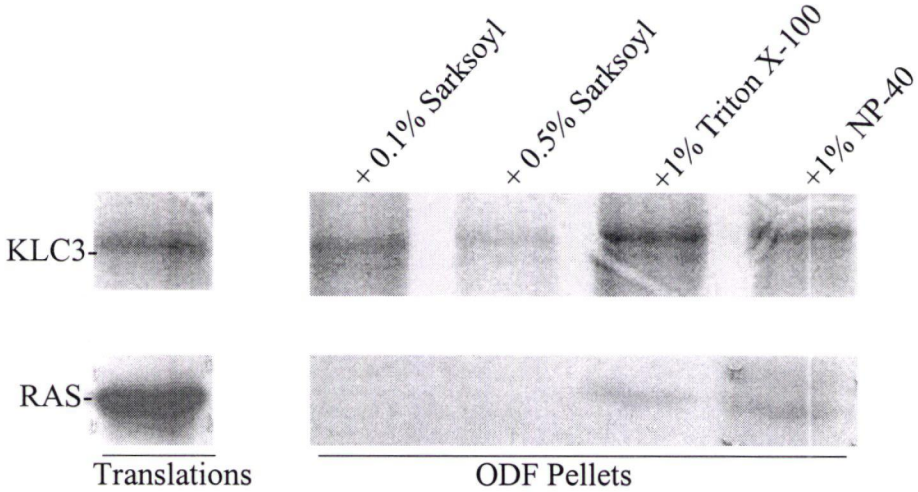
+ 0.1% Sarksoyl
+ 0.5% Sarksoyl
+1% Triton X-100
+1% NP-40
KLC3-
RAS-
Translations
ODF Pellets

To investigate the molecular basis of the KLC3-ODF binding, I next exploited the *in vitro* binding assay to delineate KLC3 sequences involved in ODF binding; deletion mutants were constructed in the HR and C-terminal regions of KLC3 and analyzed in the ODF binding assay. The results show that the 52-kDa KLC3ΔHR mutant could not bind to ODFs (figure 11 *lane 6*). Deletion of the variable C-terminal sequence in the 49-kDa KLC3ΔC mutant had no significant effect on ODF binding. (compare *lanes 3* and *7* in figure 11). These results indicate that the HR domain of KLC3 is involved in ODF interaction. This is interesting in light of the fact that the HR mediates KLC-KHC binding in the context of a kinesin complex. To further address specificity, we mixed *in vitro* translated radiolabeled KLC3 and KHC proteins and subjected them to ODFs; in comparison with KLC3, KHC showed virtually no binding (figure 11, *lanes 9* and *10*). The binding levels were shown in table 3. The autoradiogram films (figure 11) were scanned and the bands intensities were quantified. 5-time amount of bands intensities in translations panel was defined to be input. The intensities of bands in ODF pellets panel were defined to be output. The ratio of output and input was determined and expressed as percentage of binding.

5.3 Specific KLC3-ODF1 Interaction Is Mediated by Leucine Zipper Motifs

ODFs contain several major proteins as well as a number of other integral proteins. The protein SDS-PAGE showed the 84kDa, 80kDa, 30kDa, 27kDa and 14kDa polypeptides in purified rat ODFs (figure 9A). Our lab have previously cloned and characterized two major ODF proteins, ODF1 (27 kDa) (van der Hoorn, 1990) and ODF2

Figure 11. The HR of KLC3 Is Involved in ODF Interaction

Purified rat ODFs were incubated with *in vitro* translated radiolabeled wild-type KLC3 (WT), the KLC3HR mutant (HR), the KLC3C mutant (C), and p21ras (RAS). After repeated washings and pelleting steps, the amount of bound KLC3 in the final pellets was analyzed by SDS-PAGE and autoradiography. Lanes 1-4 (translations) show the input amounts of *in vitro* translated radiolabeled KLC3 variants and p21ras in the different binding reactions (20% loaded). Lanes 5-8 (ODF pellets) shows the results from analysis of radiolabeled proteins in the washed ODF pellets. Radiolabeled KLC3 and KHC were mixed and incubated with purified ODFs (T; lane 9). Bound protein was analyzed (P; lane 10). Note that, whereas wild-type KLC3 and KLC3ΔC bound efficiently to pure ODFs, a mutation in the HR domain (KLC3ΔHR mutant) abolished binding.

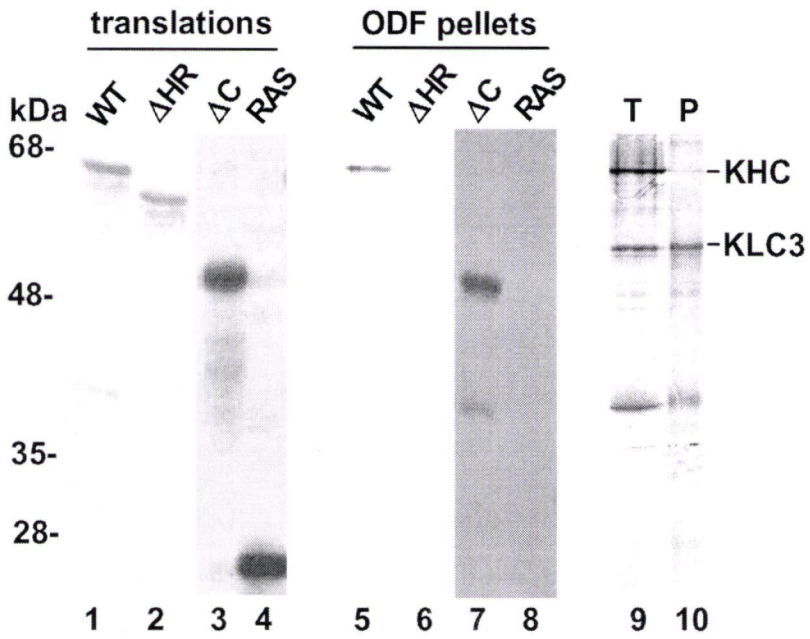
translations
ODF pellets
kDa
WT
ΔHR
ΔC
RAS
WT
ΔHR
ΔC
RAS
T
P
68-
48-
35-
28-
KHC
KLC3
1
2
3
4
5
6
7
8
9
10

Table 3 KLC3-ODF *in vitro* binding

IVT Proteins	WTKLC3	KLC3 ΔHR	KLC3ΔC	KHC	RAS
ODF Binding	18%	0	17%	2%	0

(84 kDa) (Shao, 1997). To identify which ODF protein(s), if any, bind to KLC3, our lab had carried out western blot overlay assays using radiolabeled KLC3 as a probe. Results showed that binding of KLC3 to a 27-kDa ODF protein (Bhullar, 2003). We expected it to be the 27kDa major protein ODF1. ODF1 is a multifunctional protein that contains an N-terminal leucine zipper motif that specifies binding to several ODF and ODF-associated proteins (Shao, 1997; Shao, 1999; Shao, 2001) as well as a conserved CGP repeat in the C terminus that we recently showed binds to a novel RING finger protein, OIP1 (Zarsky, 2003). To prove that ODF1 can bind KLC3 and to delineate regions in ODF1 involved in this binding, we used two different assays: the yeast two-hybrid system and a cell-free GST-ODF1 pull-down assay. In addition, because the HR domain resembles a leucine zipper motif, and because we had demonstrated that the major ODF and ODF-associated proteins interact using leucine zipper motifs, one possibility was that the KLC3 HR domain interacts with the ODF1 leucine zipper motif.

KLC3-ODF1 interaction is mediated by KLC3 HR domain

The two-hybrid system is an *in vivo* yeast-based system (derived from the yeast GAL4 protein) that identifies the interaction between two proteins by reconstituting active transcription factor dimmers. The two-hybrid plasmids were constructed as described in Materials and Methods. Each pair of the two-hybrid plasmids pGBT9/ Odf1NT and pGAD/KLC3WT, pGBT9/ Odf1CT and pGAD/KLC3WT, pGBT9/ Odf1NT and pGAD/KLC3ΔHR; pGBT9/ Odf1NT and pGAD/KLC3ΔC, pGBT9/ Odf1NT100 and pGAD/KLC3WT, was transformed into the yeast strains SFY526 (for β-

galactosidase assay) and HF7c (for His3 assay), using the small-scale yeast transformation procedure. The transformed yeast culture was spread on selective media: the transformants with the pGAD hybrid plasmid were selected on SD medium lacking leucine, while the transformants with the pGBT hybrid plasmid were selected on SD medium lacking tryptophan. β-Galactosidase filter assays were performed for SFY526 yeast strain, and His3 select assays were performed for HF7c strain. The D panel in figure 12 shows the plasmids used in this experiments. The figure 12A showed the co-transformation of the pGBT9 and pGAD plasmid constructions. Empty pGBT9 vector was used as a negative control (NO. 6). Then this plate was used as a master plate for transferring the yeast onto a filter for β-galactosidase assay (figure 12B). It showed that only pGADKLC3WT/pGBT9ODF1NT, pGADKLC3WT/pGBT9ODF1NT100 and pGADKLC3ΔC/pGBT9ODF1NT transformed yeast cells have the appearance of blue colour.

The results suggest that KLC3WT can interact with ODF1NT (No. 1) and ODFNT100 (No.2). KLC3 C terminal mutant interacts with ODF1NT (No.5). The deletion of N terminal Leucine-Zipper motif abolished the interaction with ODFNT (No.4). The results obtained in the His selection were identical with activation assays (figure 12C). More proteins were detected in yeast two-hybrid system further; all the results are summarized in table 4. These data demonstrate that (i) KLC3 can bind to ODF1, but not to ODF2, in agreement with the suggestions from the Western blot overlay assays; (ii) KLC3 associates with the N-terminal half of ODF1 (ODF1 NT), but not with

Figure 12. ODF1 can specifically associate with KLC3 in yeast

The binding of KLC3 to ODF1 was analyzed in yeast. KLC3 expression constructs were based on pGAD424, and ODF1 expression constructs were based on pGBT9 as described previously. The pGBT9 and pGAD plasmids were cotransformed into yeast strains SFY526 and HF7c.

A. For each combination, four yeast SFY256 colonies containing the indicated DNAs were plated as small horizontal streaks in SD/Leu-Trp- plate, growth and used as the master plate.

B. Filter assay for β –Galactosidase, Blue color on the filter indicated the positive interactions between the two hybrid proteins. Yeast cell were transferred from master plate to filters before carrying out the assay. ODF1NT and ODF1CT contain the N- and C-terminal halves of ODF1, respectively.

C. His 3 report assay. Growth in the absence of His was tested in yeast strain HF7c. In His growth assays, the plasmid combinations indicated in D panel were introduced in yeast strain HF7c, and colonies containing both plasmids were selected and grown as shown.

A

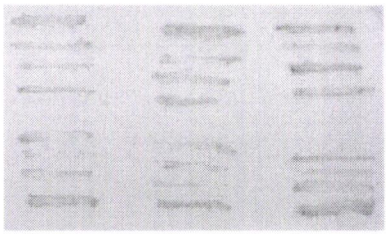

B

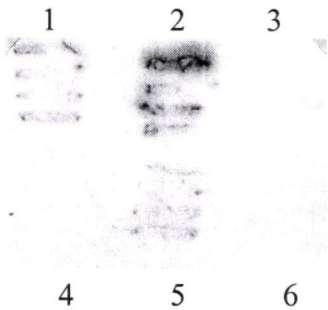

C

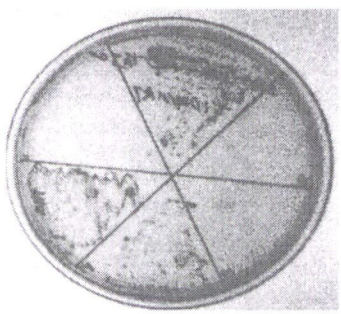

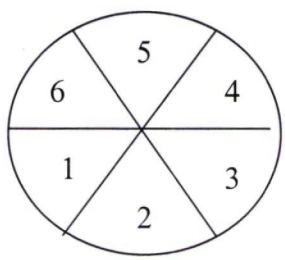

D

1.wtKLC3 ODF1NT	2.wtKLC3 ODF1NT100	3.wtKLC3 ODFCT
4. KLCΔ HR ODF1NT	5.KLC3Δ C ODF1NT	6. empty vectors

Table 4. KLC3 binding to ODF1 in yeast

pGBT construct	pGAD-KLC3	pGAD-KLC3NT	pGAD-KLC3 Δ HR	pGAD-KLC3 Δ C
ODF1NT[a]	+[b]	+	–	–
ODF1CT[c]	–	–	–	–
ODF1NT100	+	+	**ND**	**ND**
ODF2	–	–	**ND**	**ND**

[a] ODF1NT contains the N-terminal half of ODF1, which harbors the leucine zipper motif.

[b] +, protein interaction; -, lack of interaction; ND, not determined.

[c] ODF1CT contains the C-terminal half of ODF1, which harbors the conserved CGP repeats.

the C-terminal half (ODF1CT); and (iii) deletion of the KLC3 HR domain abolishes binding to ODF1, whereas deletion of the KLC3 C terminus does not affect binding. The results also show that the first 100 amino acid residues of ODF1 (ODF1NT100) suffice for KLC3 interaction. In conclusion, the yeast data demonstrate that KLC3 and ODF1 can interact directly.

KLC3-ODF1 Interaction is Mediated by ODF1 Leucine Zipper Motif

The yeast two-hybrid data suggested the N-terminal of Odf1 was involved in the association with KLC3. To confirm and extend the yeast results, I made the GST-ODF1 fragment fusion proteins and did the GST pull down assay.

Preparation of GST-ODF1 fusion proteins

The vectors for the expression of GST fusion proteins were described before (Shao, 1996). The truncated Odf1-GST fusion proteins Odf1NT, Odf1Δ NT, Odf1NT25-147, Odf1CT, Odf1ΔCT (figure 13A) were expressed in bacteria after IPTG induction. The cell lysates were then analyzed in 10% SDS PAGE. Figure 13B shows the Coomassie bright blue stain of the expected proteins.

Sarkosyl concentration optimization

In order to determine the minimal concentration of sarkosyl required for avoiding non-specific binding, optimization of the detergent concentration was performed. First, I incubated GST protein and glutathione agarose beads with *in vitro* translated ^{35}S-KLC3 WT. Then in the wash buffer, I added different amounts of Sarkosyl solution to make the final concentration to be 0.01%, 0.025%, 0.05% and 0.1%. After washing, the agarose

Figure 13. GST fusion proteins expression

A shows the different ODF1 fragments that were linked to GST. Odf1NT25-147, Odf1CT and Odf1ΔCT fragments lack the leucine zipper motifs in N terminal. These fusion proteins were induced by IPTG and expressed in bacteria. B shows the expression cell lysate analysis in 10% SDS PAGE. The black stars mark the expressed GST-fusion proteins.

A

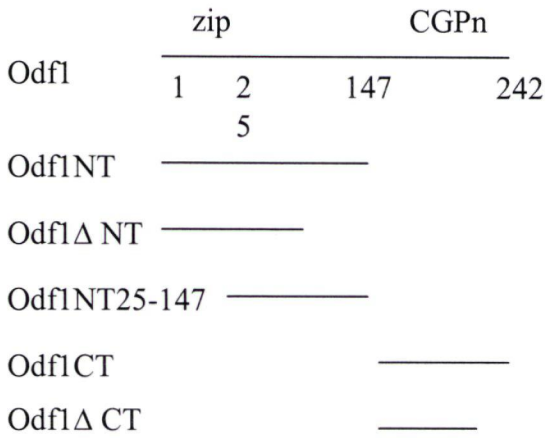
zip
CGPn
Odf1
1
2
5
147
242
Odf1NT
Odf1Δ NT
Odf1NT25-147
Odf1CT
Odf1Δ CT

B

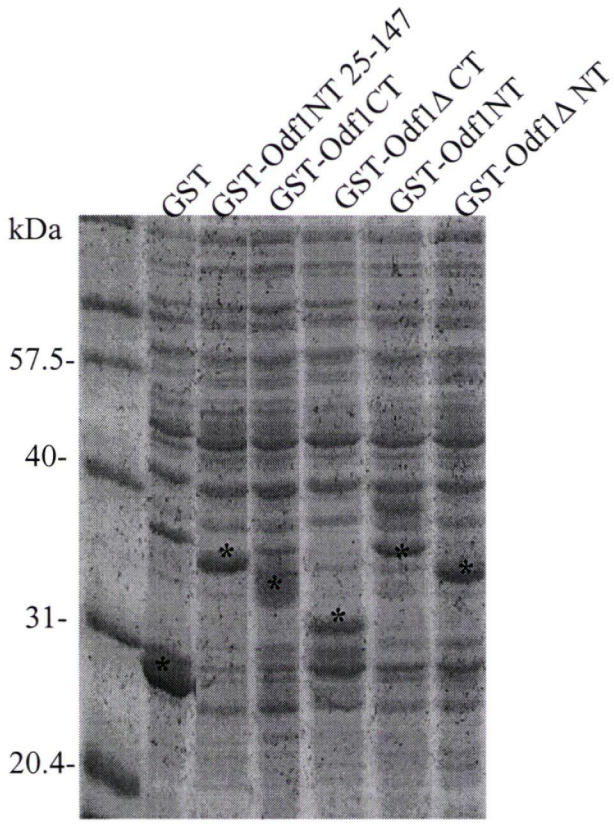
GST
GST-Odf1NT 25-147
GST-Odf1CT
GST-Odf1Δ CT
GST-Odf1NT
GST-Odf1Δ NT
kDa
57.5-
40-
31-
20.4-

Figure 14. GST fusion protein pull down assay- sarkosyl concentration optimization

GST protein and glutathione agrose beads were incubated with *in vitro* translated ^{35}S-KLC3 WT. Different amount of sarkosyl were added in the wash buffer, After wash, the beads were incubated with 2XSDS loading buffer. Then analyzed the elution proteins in SDS-PAGE and autoradiogram. The A panel shows the autoradiography KLC3 signal in Kada film, and B is the Coomassie blue gel which shows the amount of GST protein associated with beads.

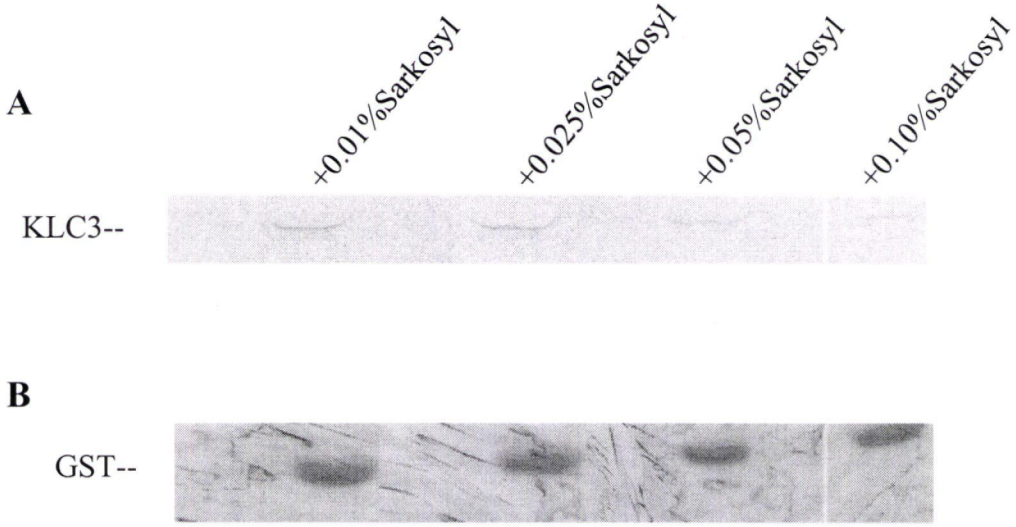
A
+0.01%Sarkosyl
+0.025%Sarkosyl
+0.05%Sarkosyl
+0.10%Sarkosyl
KLC3--
B
GST--

beads were incubated with 2XSDS loading buffer. The A panel in figure 14 shows the KLC3 signal in co-precipitation pellets and B is the Coomassie blue stained SDS-PAGE which shows the GST protein associated with beads. These results suggest that adding 0.05% sarkosyl in wash buffer decrease the non-specific binding significantly.

The N terminal Leucine zipper motif of ODF1 is involved in the KLC3-ODF1 interaction.

In order to find out which region of Odf1 is involved in the KLC3 binding, protein-protein association assays were carried out using truncated Odf1-GST fusion proteins (figure 13A). The truncated Odf1 fusion proteins were individually included in the *in vitro* translated ^{35}S KLC3. The GST fusion proteins can bind to glutathione agarose beads, so if GST fusion proteins could specifically bind to KLC3, the radiolabeled KLC3 protein could co-precipitate with agarose bead. Bound KLC3 was eluted and analyzed by SDS-PAGE and autoradiography, and the binding was quantitated. The results in figure 15A show a Coomassie-stained gel for quantitation of the amount of GST fusion proteins bind glutathione agarose beads. Figure 15B shows the autoradiogram of bound KLC3. For quantitation of binding results, the bands in figure 15A were normalized for input GST fusion protein and calculated the related interaction levels as shown is C panel. These results show that KLC3 did not bind GST, as in figure 14. KLC3 bound efficiently *in vitro* to the ODF1 N-terminal half, but not to the ODF1 C-terminal half or a deletion variant of the C-terminal half (GST-ODF1CT) that removes most of the CGP repeats, in agreement with the results in yeast. Importantly, deletion of the ODF1 leucine zipper (GST-ODF1NT25-147) significantly decreased KLC3 binding to 5% of wild-type KLC3 binding. The first 100 amino acid residues in ODF1 N-terminal

Figure 15. The Odf1 leucine zipper is involved in KLC3 binding

To analyze Odf1 sequences that mediate binding to the HR domain of KLC3, GST-Odf1 fusion protein pull-down assays were carried out. GST-Odf1NT, GSTOdf1ΔNT, GST-Odf1NT25-147, GST-Odf1CT and GST-Odf1ΔCT were incubated with *in vitro* translated radiolabeled KLC3. A shows the fusion proteins used in these experiments after separation by SDS-PAGE and staining with Coomassie. B shows the corresponding autoradiogram. The bands in B were quantitated and normalized for the different amounts of GST-Odf1 proteins used in the experiments (see A), resulting in the relative binding numbers shown in C panel (binding to Odf1NT was set arbitrarily at 100%).

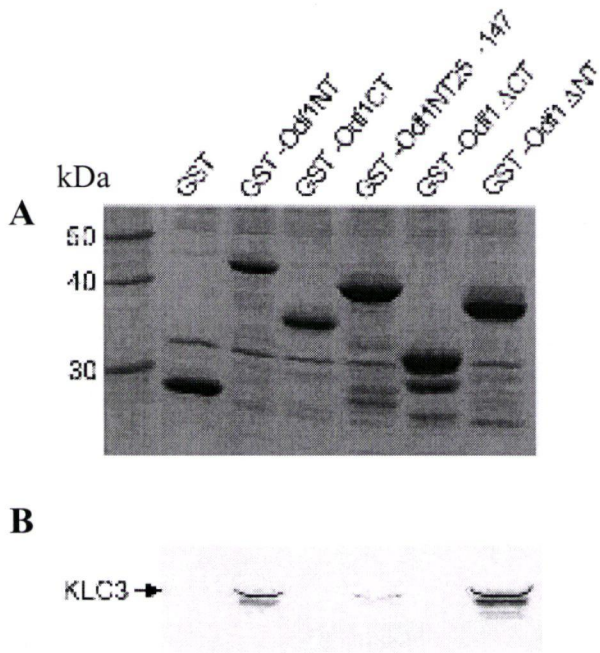

C. Relative levels of the associated KLC3 protein

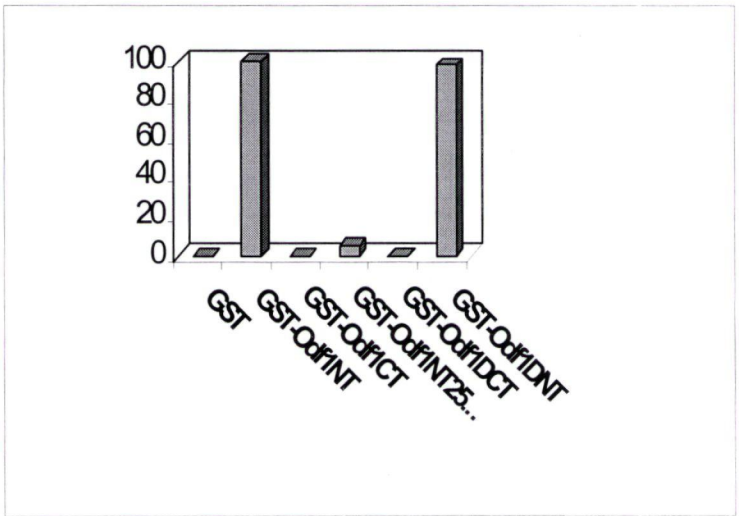

half (GST-ODF1NT) bound KLC3 with the same efficiency as wild-type KLC3.

Together, the binding experiments positively identify ODF1 as the ODF protein that binds KLC3. Moreover, this interaction is mediated by the KLC3 HR and ODF1 leucine zipper motif.

CHAPTER VI: DISCUSSION

Conventional kinesins are heterotetrameric mechanoenzymes that consist of two heavy chains and two light chains (Johnson, 1990; Kuznetsov, 1988). They are abundant and have been detected in virtually all cell types. Kinesins bind to and move along microtubules toward the plus end with few exceptions, such as the KRP NCD (Amos, 1997). Most work has concentrated on the motor domain-containing KHC proteins, which share motifs with the myosin head (Block, 1998). The globular motor domain is linked to a coiled-coil tail domain responsible for dimerization. The C terminus of KHC interacts with the HR domain in the N terminus of KLC (Hirokawa, 1989; Hackney, 1996). Because kinesins and KRPs bind microtubules, it was proposed and later demonstrated that they function in movement of organelles associated with axons, the axoneme, and mitotic spindles (Signor 2000; Diez, 2002). Kinesins and KRPs are also involved in spindle assembly and maintenance, attachment of microtubules to chromosomes, and chromosome movement (Hirokawa, 1998; Sharp, 2000, Wild, 2001). In contrast to KHC and KRPs, little is known about the interacting partner of conventional kinesins, KLC. Two roles have been postulated for KLCs.

First, as a component of kinesin, KLCs mediate the interaction between microtubules, kinesin, and membrane surfaces, including vesicles (Stenoien, 1997), microsomes (Yu, 1992), mitochondria (Khodjakov, 1998), and the trans-Golgi network (Gyoeva, 2000). Two regions in KLCs have been proposed for interaction with cargo: the conserved TPR domain and variously C terminus. Antibodies inhibit fast axonal transport without affecting microtubule binding or ATPase activity *in vitro* and cause release of purified membrane vesicles from kinesin (Stenoien, 1997). The divergent C terminus of KLC has been proposed to function as an attachment site for organelles to be transported

along microtubules (Khodjakov, 1998; Gyoeva, 2000). Second, KLC appears to regulate kinesin activity. Upon binding of KHC to KLC, KHC is released from microtubules and is kept in an inactive state by interaction between the tail and motor domains of KHC. Verhey (Verhey, 1998) hypothesized that cargo binding triggers a conformational change resulting in microtubule binding of the activated kinesin.

As described before, several kinesins and KRPs have been detected in sperm, including kinesin associated with the manchette, a transient microtubule structure (Yamazaki, 1996); KRPs (Zou 2002; Sperry, 1996); kinesin II, a KIF3-based motor molecule (Miller, 1999); and KAP3 (Yamazaki, 1996). It is important to note that kinesin II, which was found in the midpiece, consists of two different KIF3 motor proteins linked to the dynactin component (Karcher, 2002, Deacon, 2003) and lacks conventional KLC.

From morphogenetic studies, it appears that a flagellar transport mechanism must exist in testis. First, during post-meiotic differentiation of spermatids, a membrane-bound constriction point forms called the annulus, which separates the narrow and long periaxonemal compartment from the bulk of the cytoplasm (i.e. cytoplasmic lobe). Proteins needed to form specialized components of the forming sperm tail (e.g. the FS and ODFs) must thus pass through the annulus. Second, the FS forms during spermiogenesis in a distal-to-proximal orientation; thus, FS proteins must be transported to the tip of the periaxonemal compartment to begin assembly. The axoneme, which represents the first tail structure to be formed during spermiogenesis, links the periaxonemal compartment with the cytoplasmic lobe through the annulus and thus likely provides the molecular basis for microtubule-based flagellar transport.

6.1 KLC3 Protein Can Bind to ODFs

A novel kinesin light chain, KLC3 has been cloned from rat testis in our lab. The characterization showed that KLC3 shares the HR and TPR domain with other KLCs. It interacts with KHC via its HR domain and associates with microtubules *in vitro*. Interestingly, KLC3 seems to be the only known kinesin light chain expressed in spermatid. In contrast, KLC1 and KLC2 can only be detected before meiosis in testis. Here I reported that KLC3 could associate with ODFs, one of two unique macromolecular structures in mammalian spermatozoa. In immunocytochemistry experiments using anti-KLC3 MAb B11, KLC3 protein is present in elongating spermatids from stage XIV onwards and appears to localize to the sperm tail midpiece.

The further immunoelectron microscopy experiments with the MAb showed that, in mature sperm, KLC3 associates with the surface of ODFs and is present in the space between adjacent ODFs and between mitochondria and ODFs, which are devoid of tubulins (Hermo, 1991). KLC3 is not present in the medulla of ODFs, indicating that KLC3 is not an integral ODF protein like ODF1 (Higgy, 1994; Morales, 1994) and ODF2 (Shao, 1997; Schalles, 1998). Indeed, western blot analysis of highly purified ODFs failed to detect KLC3 (figure 9B). The same experiment indicated that KHC is also not an integral ODF protein, and we also showed that KHC has low affinity (if any) for purified ODFs. However, we do not know if KHC is present on ODFs in mature sperm either as part of a kinesin or as an individual protein. The presence of KLC3 on ODFs occurs in the absence of microtubules. The MAb failed to detect KLC3 label over the axoneme or over the manchette, a microtubule-rich transient structure in elongating spermatids that binds several microtubule-associated proteins (Kierszenbaum, 2001). I

conclude that the monoclonal KLC3 epitope detected in association with the ODFs is not detectable in the association of KLC3 with microtubules in spermatids.

Next, I did the in vitro binding between in vitro translated KLC3 protein and purified rat ODF. The results show that KLC3 interacts with ODF strongly (even in the presence of 0.5% sarkosyl), but not KHC, which further confirmed our ultrastructural results. These results suggest the possibility that KLC3 may be able to carry out a microtubule-independent role in spermiogenesis.

6.2 Leucine Zipper-like Repeats Mediate KLC3-ODF1 Binding

ODF is the unique cytoskeletal structure in sperm tail. Its protein components seem to be the ODF specific. In rat spermatozoa, the ODF are composed of six major polypeptides: 30, 27.5, 20, 14.4, 84 and 80kDa proteins. My purified ODF shows the same protein pattern with reported before (Vera, 1984; Oko, 1988). ODF has the special property of being resistant to solubilization in ionic detergents because of their high content of disulfide bonds (Calvin, 1971). So far only two of the major ODF protein have been cloned, 27kDa ODF1 (Higgy, 1994, Morales, 1994) and 84kDa ODF2 (Shao, 1997; Schalles, 1998). Both of them have the leucine zipper motif(s). The N-terminal leucine zipper motif of ODF1 has been known to mediate the interaction with ODF2, Spag4 and Spag5 (Shao 1997; Shao, 2001). It has been suggested that leucine zipper has a crucial role in molecular interactions during sperm tail morphogenesis.

We investigated the mechanism that KLC3 employs to bind to ODFs. First, a new ODF binding assay showed that the HR domain of KLC3 is involved in the ODF association. This is interesting because, in kinesin-based cargo transport, the KLC HR

domain (a leucine zipper like motif) interacts with KHC, and cargo associates with the variable KLC C terminus or part of the tetratricopeptide repeats. We found that deletion of the C terminus has no effect on ODF binding. Our findings imply that ODFs cannot be categorized as regular cargo for transport.

Our yeast two hybrid and GST fusion protein binding experiments uncovered that KLC3 binds directly to ODF1 and that it employs its HR sequence in this interaction. Our data predicted that the leucine zipper of ODF1 is involved in KLC3 binding. Indeed, deletion of the ODF1 leucine zipper significantly reduced binding (20-fold) to KLC3. The specificity of these leucine zipper-mediated interactions is underscored by our observation that KLC3 does not bind to ODF2 even though ODF2 contains two functional leucine zipper motifs (Shao, 1997; Kierszenbaum, 2001b). These results suggest that molecular basis for KLC3-ODF binding is the interaction of KLC3 to one of the ODF major proteins, ODF1.

6.3 Role for KLC3 in organization of structural components of the sperm tail

As mentioned in the literature review, KLC1 is mostly neuronal and KLC2 is ubiquitous (Rahman, 1998). In brain, both KLC1 and KLC2 can be detected, but their expression does differ by cell type. It has been expected that individual KLC isoforms differ in their specific cellular function. The observation that KLC3 is the only one of three known light chains to be expressed in spermatids (Junco, 2001) provides stronger evidence for the expectation. It has been suggested previously that, in addition to its ability to carry cargo down the sperm tail axoneme in the context of a kinesin-microtubule interaction in cytoplasm, KLC3 must fulfill unique spermatid-specific roles.

Indeed, the MAb used in this study indicates that KLC3 localizes to ODFs, suggestive of a spermatid-specific role. What is the nature of this binding and what could such a role(s) be?

The results described here suggest the intriguing possibility that KLC3 proteins can bind to spermatid ODFs in a microtubule-independent manner. The data in support of this possibility are the following. (i) The areas surrounding ODFs where KLC3 peptides are detected by mAbs in mature sperm are devoid of microtubules; (ii) the ODF preparations used in the *in vitro* binding assays do not contain β-tubulin; (iii) KLC3 can bind directly to ODF1 in yeast; and (iv) ODF1 and purified ODFs bind to the HR motif in KLC3, a motif normally used for binding KHC to form kinesins, not for interacting with cargo. Occupancy of the KLC3 HR motif by ODF1 will likely exclude KHC from binding to the same sequence. Based on these and previous results, we propose that, in spermatids, distinct KLC3-KHC kinesin complexes as well as KLC3-ODF1 complexes exist. The former likely act in a kinesin-mediated cargo transport in cytoplasm, whereas the latter may carry out a spermatid-specific function. A model of KLC3 roles in spermiogenesis is shown in figure 16. In A, KLC3 associates with membrane bound cargo via its TPR domain and binds KHC tail via HR motif. Then KHC binds to and moves along microtubules toward the plus end. B shows the KLC3-ODF1 complex model. KLC3 associates with membrane bound anchor (i.e. mitochondria) via its TPR domain as in A. Instead of binding to KHC, KLC3 HR domain interacts with ODF1.

A role for KLC3-ODF complexes must take into account the development of major elongating spermatid structures. The mammalian spermatozoa are free and motile

Figure 16. A model of KLC3 role in spermiogenesis

In spermiogenesis, KLC3-KHC kinesin complex as well as KLC3-ODF1 complex is proposed to exist. A: KLC3-KHC complex act in paradigm kinesin-mediated cargo transport. KLC3 associates with membrane bound cargo via its TPR domain and binds KHC C-terminal via HR motif. B: KLC3-ODF1 complex may carry out a spermatid-specific function in the development of elongating spermatid structures. KLC3 associates with membrane bound structure (i.e. mitochondria) via its TPR domain as in model A. Instead of binding to KHC, KLC3 HR domain interacts with ODF1, the major protein of ODF.

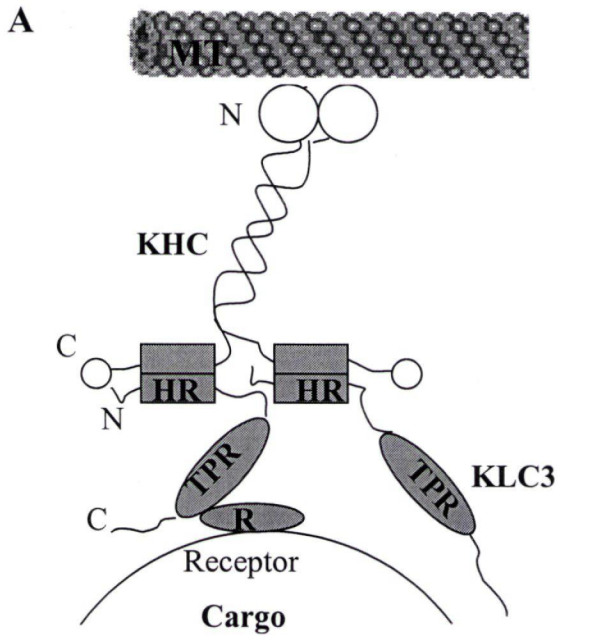
A
MT
N
KHC
C
HR
HR
N
TPR
TPR
KLC3
C
R
Receptor
Cargo

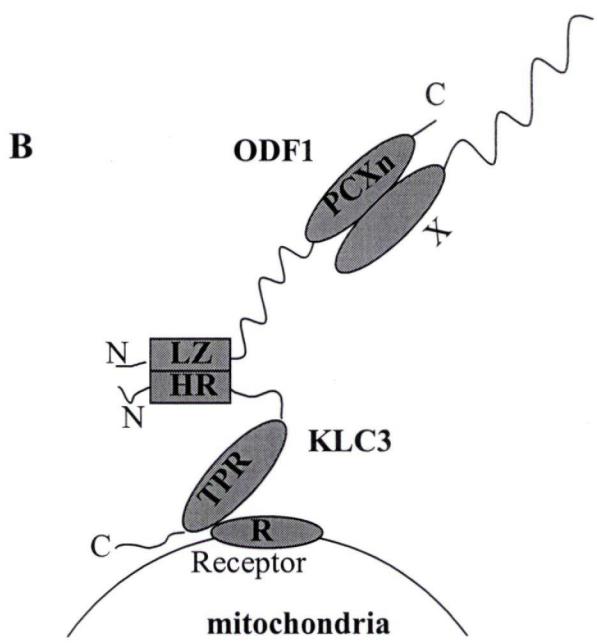
B
C
ODF1
PCXn
X
N
LZ
HR
N
KLC3
TPR
R
C
Receptor
mitochondria

cells composed of heads and tails. In sperm tail, there are several spermatids specific structures including the mitochondria sheath in the middle piece and fibrous sheath in the principal piece. Mitochondria sheath and FS are attached to the ODF and the molecular mechanisms of their biogenesis are still uncertain.

One intriguing possible role for KLC3-ODF complexes was suggested by the MAb immunocytochemistry experiments. A redistribution of mitochondria from the periphery of spermatids to the axonemal region just below the sperm head, the future midpiece, occurs in step 15-16 spermatids, a developmental stage that coincides with high level expression of KLC3 and a change in localization of KLC3 from a general cytoplasmic one to one in the sperm tail midpiece. In agreement, we observed KLC3 label between ODFs and mitochondria. We recently found that KLC3 can bind to and cluster mitochondria and that this activity depends on a region different from the HR. In the context of a possible role for KLC3 in mitochondrial ODF interactions, the following interesting observation has been made: hpy (hydrocephalic-polydactyl) mutation mice, which lack normal axonemal development during spermiogenesis, contain immature spermatids that harbor aggregates of mitochondria clustered around pieces of ODFs (Bryan, 1977). This demonstrates that normal axonemal morphogenesis is a prerequisite for tail development, and it also indicates that, in the absence of the axoneme, mitochondria can still redistribute to ODFs. We propose that KLC3 might be involved in aspects of the mitochondrial redistribution and organization.

CHAPTER VII: CONCLUSION

The electron microscopy experiments using KLC3 MAb and *in vitro* binding assay suggest that KLC3 can bind to spermatid ODFs in a microtubule -independent manner. I also investigated the mechanism that KLC3 employs to bind to ODFs. The yeast two-hybrid assay and GST fusion protein assay showed that KLC3 could bind directly to ODF1 via their leucine zipper motifs. Together with the *in vitro* binding results suggest that KLC3 HR domain (has leucine zipper motif) of KLC3 is involved in the ODF association, these results suggest that the interaction of KLC3 to ODF1 is the molecular basis for KLC3-ODF binding. The KLC3-ODF complexes exist in sperm tail indicates that KLC3 may carry out a spermatid-specific function, which is microtubule independent and might be involved in organization of structural components in the sperm tail.

References

Amos,L.A. and Cross,R.A. (1997). Structure and dynamics of molecular motors. Curr. Opin. Struct. Biol. *7*, 239-246.

Baccetti,B. (1986). Evolutionary trends in sperm structure. Comp Biochem. Physiol A *85*, 29-36.

Beushausen,S., Kladakis,A., and Jaffe,H. (1993). Kinesin light chains: identification and characterization of a family of proteins from the optic lobe of the squid Loligo pealii. DNA Cell Biol. *12*, 901-909.

Bhullar,B., Zhang,Y., Junco,A., Oko,R., and van der Hoorn,F.A. (2003). Association of kinesin light chain with outer dense fibers in a microtubule-independent fashion. J. Biol. Chem. *278*, 16159-16168.

Block,S.M. (1998). Leading the procession: new insights into kinesin motors. J. Cell Biol. *140*, 1281-1284.

Bloom,G.S. and Endow,S.A. (1995). Motor proteins 1: kinesins. Protein Profile. *2*, 1105-1171.

Bloom,G.S., Wagner,M.C., Pfister,K.K., and Brady,S.T. (1988). Native structure and physical properties of bovine brain kinesin and identification of the ATP-binding subunit polypeptide. Biochemistry *27*, 3409-3416.

Bowman,A.B., Kamal,A., Ritchings,B.W., Philp,A.V., McGrail,M., Gindhart,J.G., and Goldstein,L.S. (2000). Kinesin-dependent axonal transport is mediated by the sunday driver (SYD) protein. Cell *103*, 583-594.

Brendza,R.P., Serbus,L.R., Duffy,J.B., and Saxton,W.M. (2000). A function for kinesin I in the posterior transport of oskar mRNA and Staufen protein. Science *289*, 2120-2122.

Brohmann,H., Pinnecke,S., and Hoyer-Fender,S. (1997). Identification and characterization of new cDNAs encoding outer dense fiber proteins of rat sperm. J. Biol. Chem. *272*, 10327-10332.

Bryan, J.H., (1977). Spermatogenesis revisited. IV. Abnormal spermiogenesis in mice homozygous for another male-sterility-inducing mutation, hpy (hydrocephalic-polydactyl). Cell Tissue Res.180, 187-201.

Burfeind,P. and Hoyer-Fender,S. (1991). Sequence and developmental expression of a mRNA encoding a putative protein of rat sperm outer dense fibers. Dev. Biol. *148*, 195-204.

Cabeza-Arvelaiz,Y., Shih,L.C., Hardman,N., Asselbergs,F., Bilbe,G., Schmitz,A., White,B., Siciliano,M.J., and Lachman,L.B. (1993). Cloning and genetic characterization of the human kinesin light-chain (KLC) gene. DNA Cell Biol. *12*, 881-892.

Calvin,H.I. (1976). Isolation of subfractionation of mammalian sperm heads and tails. Methods Cell Biol. *13*, 85-104.

Calvin,H.I. (1979). Electrophoretic evidence for the identity of the major zinc-binding polypeptides in the rat sperm tail. Biol. Reprod. *21*, 873-882.

Calvin,H.I. and Bedford,J.M. (1971). Formation of disulphide bonds in the nucleus and accessory structures of mammalian spermatozoa during maturation in the epididymis. J. Reprod. Fertil. Suppl *13*, Suppl-75.

Calvin,H.I. and Bleau,G. (1974). Zinc-thiol complexes in keratin-like structures of rat spermatozoa. Exp. Cell Res. *86*, 280-284.

Clermont, Y., (1966). Renewal of spermatogonia in man. American Journal of Anatomy. 118:509

Clermont,Y., Oko,R., and Hermo,L. (1990). Immunocytochemical localization of proteins utilized in the formation of outer dense fibers and fibrous sheath in rat spermatids: an electron microscope study. Anat. Rec. *227*, 447-457.

Cole,D.G., Diener,D.R., Himelblau,A.L., Beech,P.L., Fuster,J.C., and Rosenbaum,J.L. (1998). Chlamydomonas kinesin-II-dependent intraflagellar transport (IFT): IFT particles contain proteins required for ciliary assembly in Caenorhabditis elegans sensory neurons. J. Cell Biol. *141*, 993-1008.

Collins,C.A. and Vallee,R.B. (1989). Preparation of microtubules from rat liver and testis: cytoplasmic dynein is a major microtubule associated protein. Cell Motil. Cytoskeleton *14*, 491-500.

Cyr,J.L., Pfister,K.K., Bloom,G.S., Slaughter,C.A., and Brady,S.T. (1991). Molecular genetics of kinesin light chains: generation of isoforms by alternative splicing. Proc. Natl. Acad. Sci. U. S A *88*, 10114-10118.

de Cuevas,M., Tao,T., and Goldstein,L.S. (1992). Evidence that the stalk of Drosophila kinesin heavy chain is an alpha-helical coiled coil. J. Cell Biol. *116*, 957-965.

Deacon,S.W., Serpinskaya,A.S., Vaughan,P.S., Lopez,F.M., Vernos,I., Vaughan,K.T., and Gelfand,V.I. (2003). Dynactin is required for bidirectional organelle transport. J. Cell Biol. *160*, 297-301.

Diefenbach,R.J., Mackay,J.P., Armati,P.J., and Cunningham,A.L. (1998). The C-terminal region of the stalk domain of ubiquitous human kinesin heavy chain contains the binding site for kinesin light chain. Biochemistry *37*, 16663-16670.

Diez,S., Schief,W.R., and Howard,J. (2002). Molecular motors: single-molecule recordings made easy. Curr. Biol. *12*, R203-R205.

Dym M., and Clermont Y., (1970). Role of spermatogonia in the repair of the seminiferous epithelium following X-irradiation of the rat testis. American journal of Anatomy. 128:265-281.

Elluru,R.G., Bloom,G.S., and Brady,S.T. (1995). Fast axonal transport of kinesin in the rat visual system: functionality of kinesin heavy chain isoforms. Mol. Biol. Cell *6*, 21-40.

Fan,J. and Amos,L.A. (1994). Kinesin light chain isoforms in Caenorhabditis elegans. J. Mol. Biol. *240*, 507-512.

Fawcett,D.W. (1975). The mammalian spermatozoon. Dev. Biol. *44*, 394-436.

Fontaine,J.M., Rest,J.S., Welsh,M.J., and Benndorf,R. (2003). The sperm outer dense fiber protein is the 10th member of the superfamily of mammalian small stress proteins. Cell Stress. Chaperones. *8*, 62-69.

Frangioni,J.V. and Neel,B.G. (1993). Solubilization and purification of enzymatically active glutathione S-transferase (pGEX) fusion proteins. Anal. Biochem. *210*, 179-187.

Gastmann,O., Burfeind,P., Gunther,E., Hameister,H., Szpirer,C., and Hoyer-Fender,S. (1993). Sequence, expression, and chromosomal assignment of a human sperm outer dense fiber gene. Mol. Reprod. Dev. *36*, 407-418.

Gauger,A.K. and Goldstein,L.S. (1993). The Drosophila kinesin light chain. Primary structure and interaction with kinesin heavy chain. J. Biol. Chem. *268*, 13657-13666.

Gelfand,V.I., Le Bot,N., Tuma,M.C., and Vernos,I. (2001). A dominant negative approach for functional studies of the kinesin II complex. Methods Mol. Biol. *164*, 191-204.

Gindhart,J.G., Jr., Desai,C.J., Beushausen,S., Zinn,K., and Goldstein,L.S. (1998). Kinesin light chains are essential for axonal transport in Drosophila. J. Cell Biol. *141*, 443-454.

Gindhart,J.G., Jr. and Goldstein,L.S. (1996). Tetratrico peptide repeats are present in the kinesin light chain. Trends Biochem. Sci. *21*, 52-53.

Goldstein,L.S. (2001a). Kinesin molecular motors: transport pathways, receptors, and human disease. Proc. Natl. Acad. Sci. U. S A *98*, 6999-7003.

Goldstein,L.S. (2001b). Molecular motors: from one motor many tails to one motor many tales. Trends Cell Biol. *11*, 477-482.

Goldstein,L.S. and Philp,A.V. (1999). The road less traveled: emerging principles of kinesin motor utilization. Annu. Rev. Cell Dev. Biol. *15*, 141-183.

Goldstein,L.S. and Yang,Z. (2000). Microtubule-based transport systems in neurons: the roles of kinesins and dyneins. Annu. Rev. Neurosci. *23*, 39-71.

Gyoeva,F.K., Bybikova,E.M., and Minin,A.A. (2000). An isoform of kinesin light chain specific for the Golgi complex. J. Cell Sci. *113 (Pt 11)*, 2047-2054.

Hackney,D.D. (1996). The kinetic cycles of myosin, kinesin, and dynein. Annu. Rev. Physiol *58*, 731-750.

Hall,E.S., Eveleth,J., Jiang,C., Redenbach,D.M., and Boekelheide,K. (1992). Distribution of the microtubule-dependent motors cytoplasmic dynein and kinesin in rat testis. Biol. Reprod. *46*, 817-828.

Hall,E.S., Hall,S.J., and Boekelheide,K. (1995). 2,5-Hexanedione exposure alters microtubule motor distribution in adult rat testis. Fundam. Appl. Toxicol. *24*, 173-182.

Henkel,R., Stalf,T., and Miska,W. (1992). Isolation and partial characterization of the outer dense fiber proteins from human spermatozoa. Biol. Chem. Hoppe Seyler *373*, 685-689.

Henson,J.H., Cole,D.G., Roesener,C.D., Capuano,S., Mendola,R.J., and Scholey,J.M. (1997). The heterotrimeric motor protein kinesin-II localizes to the midpiece and flagellum of sea urchin and sand dollar sperm. Cell Motil. Cytoskeleton *38*, 29-37.

Hermo,L., Oko,R., and Hecht,N.B. (1991). Differential post-translational modifications of microtubules in cells of the seminiferous epithelium of the rat: a light and electron microscope immunocytochemical study. Anat. Rec. *229*, 31-50.

Higgy,N.A., Pastoor,T., Renz,C., Tarnasky,H.A., and van der Hoorn,F.A. (1994). Testis-specific RT7 protein localizes to the sperm tail and associates with itself. Biol. Reprod. *50*, 1357-1366.

Hirokawa,N. (1996). The molecular mechanism of organelle transport along microtubules: the identification and characterization of KIFs (kinesin superfamily proteins). Cell Struct. Funct. *21*, 357-367.

Hirokawa,N. (1998). Kinesin and dynein superfamily proteins and the mechanism of organelle transport. Science *279*, 519-526.

Hirokawa,N., Pfister,K.K., Yorifuji,H., Wagner,M.C., Brady,S.T., and Bloom,G.S. (1989). Submolecular domains of bovine brain kinesin identified by electron microscopy and monoclonal antibody decoration. Cell *56*, 867-878.

Hollenbeck,P.J. (1989). The distribution, abundance and subcellular localization of kinesin. J. Cell Biol. *108*, 2335-2342.

Hollenbeck,P.J. (1993). Phosphorylation of neuronal kinesin heavy and light chains in vivo. J. Neurochem. *60*, 2265-2275.

Howard,J. and Hyman,A.A. (2003). Dynamics and mechanics of the microtubule plus end. Nature *422*, 753-758.

Hoyer-Fender,S., Burfeind,P., and Hameister,H. (1995). Sequence of mouse Odf1 cDNA and its chromosomal localization: extension of the linkage group between human chromosome 8 and mouse chromosome 15. Cytogenet. Cell Genet. *70*, 200-204.

Hoyer-Fender,S., Petersen,C., Brohmann,H., Rhee,K., and Wolgemuth,D.J. (1998). Mouse Odf2 cDNAs consist of evolutionary conserved as well as highly variable sequences and encode outer dense fiber proteins of the sperm tail. Mol. Reprod. Dev. *51*, 167-175.

Irons,M.J. and Clermont,Y. (1982). Formation of the outer dense fibers during spermiogenesis in the rat. Anat. Rec. *202*, 463-471.

Ito,M., Yoshioka,K., Akechi,M., Yamashita,S., Takamatsu,N., Sugiyama,K., Hibi,M., Nakabeppu,Y., Shiba,T., and Yamamoto,K.I. (1999). JSAP1, a novel jun N-terminal protein kinase (JNK)-binding protein that functions as a Scaffold factor in the JNK signaling pathway. Mol. Cell Biol. *19*, 7539-7548.

Johnson,C.S., Buster,D., and Scholey,J.M. (1990). Light chains of sea urchin kinesin identified by immunoadsorption. Cell Motil. Cytoskeleton *16*, 204-213.

Johnson,K.J., Hall,E.S., and Boekelheide,K. (1996). Kinesin localizes to the trans-Golgi network regardless of microtubule organization. Eur. J. Cell Biol. *69*, 276-287.

Junco,A., Bhullar,B., Tarnasky,H.A., and van der Hoorn,F.A. (2001). Kinesin light-chain KLC3 expression in testis is restricted to spermatids. Biol. Reprod. *64*, 1320-1330.

Kamal,A. and Goldstein,L.S. (2002). Principles of cargo attachment to cytoplasmic motor proteins. Curr. Opin. Cell Biol. *14*, 63-68.

Kamal,A., Stokin,G.B., Yang,Z., Xia,C.H., and Goldstein,L.S. (2000). Axonal transport of amyloid precursor protein is mediated by direct binding to the kinesin light chain subunit of kinesin-I. Neuron *28*, 449-459.

Kanai,Y., Okada,Y., Tanaka,Y., Harada,A., Terada,S., and Hirokawa,N. (2000). KIF5C, a novel neuronal kinesin enriched in motor neurons. J. Neurosci. *20*, 6374-6384.

Kappe,G., Franck,E., Verschuure,P., Boelens,W.C., Leunissen,J.A., and de Jong,W.W. (2003). The human genome encodes 10 alpha-crystallin-related small heat shock proteins: HspB1-10. Cell Stress. Chaperones. *8*, 53-61.

Karcher,R.L., Deacon,S.W., and Gelfand,V.I. (2002). Motor-cargo interactions: the key to transport specificity. Trends Cell Biol. *12*, 21-27.

Kashina,A.S., Rogers,G.C., and Scholey,J.M. (1997). The bimC family of kinesins: essential bipolar mitotic motors driving centrosome separation. Biochim. Biophys. Acta *1357*, 257-271.

Khodjakov,A., Lizunova,E.M., Minin,A.A., Koonce,M.P., and Gyoeva,F.K. (1998). A specific light chain of kinesin associates with mitochondria in cultured cells. Mol. Biol. Cell *9*, 333-343.

Kierszenbaum,A.L. (2001a). Spermatid manchette: plugging proteins to zero into the sperm tail. Mol. Reprod. Dev. *59*, 347-349.

Kierszenbaum,A.L. (2001b). Transition nuclear proteins during spermiogenesis: unrepaired DNA breaks not allowed. Mol. Reprod. Dev. *58*, 357-358.

Kierszenbaum,A.L. (2002a). Intramanchette transport (IMT): managing the making of the spermatid head, centrosome, and tail. Mol. Reprod. Dev. *63*, 1-4.

Kierszenbaum,A.L. (2002b). Keratins: unraveling the coordinated construction of scaffolds in spermatogenic cells. Mol. Reprod. Dev. *61*, 1-2.

Kim,Y., Adham,I.M., Haack,T., Kremling,H., and Engel,W. (1995). Molecular cloning and characterization of the bovine and porcine outer dense fibers cDNA and organization of the bovine gene. Biol. Chem. Hoppe Seyler *376*, 431-435.

Kuhn,R., Kuhn,C., Borsch,D., Glatzer,K.H., Schafer,U., and Schafer,M. (1991). A cluster of four genes selectively expressed in the male germ line of Drosophila melanogaster. Mech. Dev. *35*, 143-151.

Kull,F.J. (2000). Motor proteins of the kinesin superfamily: structure and mechanism. Essays Biochem. *35*, 61-73.

Kuznetsov,S.A., Vaisberg,E.A., Shanina,N.A., Magretova,N.N., Chernyak,V.Y., and Gelfand,V.I. (1988). The quaternary structure of bovine brain kinesin. EMBO J. *7*, 353-356.

Kuznetsov,S.A., Vaisberg,Y.A., Rothwell,S.W., Murphy,D.B., and Gelfand,V.I. (1989). Isolation of a 45-kDa fragment from the kinesin heavy chain with enhanced ATPase and microtubule-binding activities. J. Biol. Chem. *264*, 589-595.

Lamerdin,J.E., Stilwagen,S.A., Ramirez,M.H., Stubbs,L., and Carrano,A.V. (1996). Sequence analysis of the ERCC2 gene regions in human, mouse, and hamster reveals three linked genes. Genomics *34*, 399-409.

Marshall,J. and Holberton,D.V. (1995). Giardia gene predicts a 183 kDa nucleotide-binding head-stalk protein. J. Cell Sci. *108 (Pt 7)*, 2683-2692.

Marszalek,J.R. and Goldstein,L.S. (2000). Understanding the functions of kinesin-II. Biochim. Biophys. Acta *1496*, 142-150.

Miki, H., Setou. M., Kaneshiro, K. and Hirokawa, N. (2001). All kinesin superfamily protein, KIF genes in mouse and human. Proc Natl Acad Sci U S A. 98, 7004-11.

Miller,M.G., Mulholland,D.J., and Vogl,A.W. (1999). Rat testis motor proteins associated with spermatid translocation (dynein) and spermatid flagella (kinesin-II). Biol. Reprod. *60*, 1047-1056.

Morales,C.R., Oko,R., and Clermont,Y. (1994). Molecular cloning and developmental expression of an mRNA encoding the 27 kDa outer dense fiber protein of rat spermatozoa. Mol. Reprod. Dev. *37*, 229-240.

Nakagawa,T., Tanaka,Y., Matsuoka,E., Kondo,S., Okada,Y., Noda,Y., Kanai,Y., and Hirokawa,N. (1997). Identification and classification of 16 new kinesin superfamily (KIF) proteins in mouse genome. Proc. Natl. Acad. Sci. U. S A *94*, 9654-9659.

Nakagawa, T., Yamane Y, Okanoue T, Tsukita S, and Tsukita S. (2001). Outer dense fiber 2 is a widespread centrosome scaffold component preferentially associated with mother centrioles: its identification from isolated centrosomes. Mol Biol Cell.12. 1687-97.

Navolanic,P.M. and Sperry,A.O. (2000). Identification of isoforms of a mitotic motor in mammalian spermatogenesis. Biol. Reprod. *62*, 1360-1369.

Neely,M.D. and Boekelheide,K. (1988). Sertoli cell processes have axoplasmic features: an ordered microtubule distribution and an abundant high molecular weight microtubule-associated protein (cytoplasmic dynein). J. Cell Biol. *107*, 1767-1776.

Niclas,J., Navone,F., Hom-Booher,N., and Vale,R.D. (1994). Cloning and localization of a conventional kinesin motor expressed exclusively in neurons. Neuron *12*, 1059-1072.

Oko,R. (1988). Comparative analysis of proteins from the fibrous sheath and outer dense fibers of rat spermatozoa. Biol. Reprod. *39*, 169-182.

Oko,R. and Clermont,Y. (1989). Light microscopic immunocytochemical study of fibrous sheath and outer dense fiber formation in the rat spermatid. Anat. Rec. *225*, 46-55.

Oko,R., Moussakova,L., and Clermont,Y. (1990). Regional differences in composition of the perforatorium and outer periacrosomal layer of the rat spermatozoon as revealed by immunocytochemistry. Am. J. Anat. *188*, 64-73.

Olson,G.E. and Sammons,D.W. (1980). Structural chemistry of outer dense fibers of rat sperm. Biol. Reprod. *22*, 319-332.

Ong, L.L., Lim, A.P., Er, C.P., Kuznetsov, S.A., and Yu, H. (2000). Kinectin-kinesin binding domains and their effects on organelle motility. J Biol Chem. 275, 32854-60.

Petersen,C., Aumuller,G., Bahrami,M., and Hoyer-Fender,S. (2002). Molecular cloning of Odf3 encoding a novel coiled-coil protein of sperm tail outer dense fibers. Molecular Reproduction and Development *61*, 102-112.

Petersen,C., Fuzesi,L., and Hoyer-Fender,S. (1999). Outer dense fibre proteins from human sperm tail: molecular cloning and expression analyses of two cDNA transcripts encoding proteins of approximately 70 kDa. Mol. Hum. Reprod. *5*, 627-635.

Piperno,G. and Mead,K. (1997). Transport of a novel complex in the cytoplasmic matrix of Chlamydomonas flagella. Proc. Natl. Acad. Sci. U. S A *94*, 4457-4462.

Rahman,A., Friedman,D.S., and Goldstein,L.S. (1998). Two kinesin light chain genes in mice. Identification and characterization of the encoded proteins. J. Biol. Chem. *273*, 15395-15403.

Rahman,A., Kamal,A., Roberts,E.A., and Goldstein,L.S. (1999). Defective kinesin heavy chain behavior in mouse kinesin light chain mutants. J. Cell Biol. *146*, 1277-1288.

Rattner,J.B. and Brinkley,B.R. (1972). Ultrastructure of mammalian spermiogenesis. 3. The organization and morphogenesis of the manchette during rodent spermiogenesis. J. Ultrastruct. Res. *41*, 209-218.

Reid,E., Kloos,M., Ashley-Koch,A., Hughes,L., Bevan,S., Svenson,I.K., Graham,F.L., Gaskell,P.C., Dearlove,A., Pericak-Vance,M.A., Rubinsztein,D.C., and Marchuk,D.A. (2002). A kinesin heavy chain (KIF5A) mutation in hereditary spastic paraplegia (SPG10). Am. J. Hum. Genet. *71*, 1189-1194.

Russell, L.D., Ettlin, R.A., Sinha Hikim, A.P., and Clegg, E.D. (1990). Histological and histopathological evalution of the testis. pp. 1-52 Cache River Press Clearwater, FL.

Sambrook, J., (1989). Molecular Cloning : a laboratory manual. Cold Spring Harbor Laboratory Press, Cold Spring Harbor, N.Y.

Saxton,W.M., Hicks,J., Goldstein,L.S., and Raff,E.C. (1991). Kinesin heavy chain is essential for viability and neuromuscular functions in Drosophila, but mutants show no defects in mitosis. Cell *64*, 1093-1102.

Schafer,M., Borsch,D., Hulster,A., and Schafer,U. (1993). Expression of a gene duplication encoding conserved sperm tail proteins is translationally regulated in Drosophila melanogaster. Mol. Cell Biol. *13*, 1708-1718.

Schalles,U., Shao,X., van der Hoorn,F.A., and Oko,R. (1998). Developmental expression of the 84-kDa ODF sperm protein: localization to both the cortex and medulla of outer dense fibers and to the connecting piece. Dev. Biol. *199*, 250-260.

Schiestl,R.H. and Gietz,R.D. (1989). High efficiency transformation of intact yeast cells using single stranded nucleic acids as a carrier. Curr. Genet. *16*, 339-346.

Seiler,S., Kirchner,J., Horn,C., Kallipolitou,A., Woehlke,G., and Schliwa,M. (2000). Cargo binding and regulatory sites in the tail of fungal conventional kinesin. Nat. Cell Biol. *2*, 333-338.

Seiler,S., Nargang,F.E., Steinberg,G., and Schliwa,M. (1997). Kinesin is essential for cell morphogenesis and polarized secretion in Neurospora crassa. EMBO J. *16*, 3025-3034.

Selkoe,D.J. (1999). Translating cell biology into therapeutic advances in Alzheimer's disease. Nature *399*, A23-A31.

Shao,X., Tarnasky,H.A., Lee,J.P., Oko,R., and van der Hoorn,F.A. (1999). Spag4, a novel sperm protein, binds outer dense-fiber protein Odf1 and localizes to microtubules of manchette and axoneme. Dev. Biol. *211*, 109-123.

Shao,X., Tarnasky,H.A., Schalles,U., Oko,R., and van der Hoorn,F.A. (1997). Interactional cloning of the 84-kDa major outer dense fiber protein Odf84. Leucine zippers mediate associations of Odf84 and Odf27. J. Biol. Chem. *272*, 6105-6113.

Shao,X. and van der Hoorn,F.A. (1996). Self-interaction of the major 27-kilodalton outer dense fiber protein is in part mediated by a leucine zipper domain in the rat. Biol. Reprod. *55*, 1343-1350.

Shao,X.P., Xue,J.P., and van der Hoorn,F.A. (2001). Testicular protein Spag5 has similarity to mitotic spindle protein deepest and binds outer dense fiber protein Odf1. Molecular Reproduction and Development *59*, 410-416.

Sharp,D.J., Rogers,G.C., and Scholey,J.M. (2000). Roles of motor proteins in building microtubule-based structures: a basic principle of cellular design. Biochim. Biophys. Acta *1496*, 128-141.

Signor,D. and Scholey,J.M. (2000). Microtubule-based transport along axons, dendrites and axonemes. Essays Biochem. *35*, 89-102.

Skoufias,D.A., Cole,D.G., Wedaman,K.P., and Scholey,J.M. (1994). The carboxyl-terminal domain of kinesin heavy chain is important for membrane binding. J. Biol. Chem. *269*, 1477-1485.

Sperry,A.O. and Zhao,L.P. (1996). Kinesin-related proteins in the mammalian testes: candidate motors for meiosis and morphogenesis. Mol. Biol. Cell *7*, 289-305.

Steinberg,G. and Schliwa,M. (1995). The Neurospora organelle motor: a distant relative of conventional kinesin with unconventional properties. Mol. Biol. Cell *6*, 1605-1618.

Stenoien,D.L. and Brady,S.T. (1997). Immunochemical analysis of kinesin light chain function. Mol. Biol. Cell *8*, 675-689.

Stock,M.F., Guerrero,J., Cobb,B., Eggers,C.T., Huang,T.G., Li,X., and Hackney,D.D. (1999). Formation of the compact confomer of kinesin requires a COOH-terminal heavy chain domain and inhibits microtubule-stimulated ATPase activity. J. Biol. Chem. *274*, 14617-14623.

Tanaka,Y., Kanai,Y., Okada,Y., Nonaka,S., Takeda,S., Harada,A., and Hirokawa,N. (1998). Targeted disruption of mouse conventional kinesin heavy chain, kif5B, results in abnormal perinuclear clustering of mitochondria. Cell *93*, 1147-1158.

Tang, W., Bell C., Sale W., and Gibbons I. (1981). Structure of the dyenin-1 outer arm in sea urchin sperm flagella. J. Biol. Chem. 257, 508-515.

Thomas,N., Imafuku,Y., Kamiya,T., and Tawada,K. (2002). Kinesin: a molecular motor with a spring in its step. Proc. R. Soc. Lond B Biol. Sci. *269*, 2363-2371.

Toyoshima, I., Yu, H., Steuer, E.R., and Sheetz, M.P. (1992). Kinectin, a major kinesin-binding protein on ER. J Cell Biol. 118,1121-1131.

Vale,R.D., Reese,T.S., and Sheetz,M.P. (1985a). Identification of a novel force-generating protein, kinesin, involved in microtubule-based motility. Cell *42*, 39-50.

Vale,R.D., Schnapp,B.J., Mitchison,T., Steuer,E., Reese,T.S., and Sheetz,M.P. (1985b). Different axoplasmic proteins generate movement in opposite directions along microtubules in vitro. Cell *43*, 623-632.

van der Hoorn,F.A., Tarnasky,H.A., and Nordeen,S.K. (1990). A new rat gene RT7 is specifically expressed during spermatogenesis. Dev. Biol. *142*, 147-154.

Vera,J.C., Brito,M., Zuvic,T., and Burzio,L.O. (1984). Polypeptide composition of rat sperm outer dense fibers. A simple procedure to isolate the fibrillar complex. J. Biol. Chem. *259*, 5970-5977.

Verhey,K.J., Lizotte,D.L., Abramson,T., Barenboim,L., Schnapp,B.J., and Rapoport,T.A. (1998). Light chain-dependent regulation of Kinesin's interaction with microtubules. J. Cell Biol. *143*, 1053-1066.

Verhey, K.J.and Rapoport, T.A., (2001). Kinesin carries the signal. Trends Biochem Sci. 9, 545-550.

Vignali,G., Lizier,C., Sprocati,M.T., Sirtori,C., Battaglia,G., and Navone,F. (1997). Expression of neuronal kinesin heavy chain is developmentally regulated in the central nervous system of the rat. J. Neurochem. *69*, 1840-1849.

Vignali,G., Niclas,J., Sprocati,M.T., Vale,R.D., Sirtori,C., and Navone,F. (1996). Differential expression of ubiquitous and neuronal kinesin heavy chains during differentiation of human neuroblastoma and PC12 cells. Eur. J. Neurosci. *8*, 536-544.

Wedaman,K.P., Knight,A.E., Kendrick-Jones,J., and Scholey,J.M. (1993). Sequences of sea urchin kinesin light chain isoforms. J. Mol. Biol. *231*, 155-158.

Welte,M.A., Gross,S.P., Postner,M., Block,S.M., and Wieschaus,E.F. (1998). Developmental regulation of vesicle transport in Drosophila embryos: forces and kinetics. Cell *92*, 547-557.

Wilde,A., Lizarraga,S.B., Zhang,L., Wiese,C., Gliksman,N.R., Walczak,C.E., and Zheng,Y. (2001). Ran stimulates spindle assembly by altering microtubule dynamics and the balance of motor activities. Nat. Cell Biol. *3*, 221-227.

Yamazaki,H., Nakata,T., Okada,Y., and Hirokawa,N. (1995). KIF3A/B: a heterodimeric kinesin superfamily protein that works as a microtubule plus end-directed motor for membrane organelle transport. J. Cell Biol. *130*, 1387-1399.

Yamazaki,H., Nakata,T., Okada,Y., and Hirokawa,N. (1996). Cloning and characterization of KAP3: a novel kinesin superfamily-associated protein of KIF3A/3B. Proc. Natl. Acad. Sci. U. S A *93*, 8443-8448.

Yang,J., Liu,X., Yue,G., Adamian,M., Bulgakov,O., and Li,T. (2002). Rootletin, a novel coiled-coil protein, is a structural component of the ciliary rootlet. J. Cell Biol. *159*, 431-440.

Yang,J.T., Laymon,R.A., and Goldstein,L.S. (1989). A three-domain structure of kinesin heavy chain revealed by DNA sequence and microtubule binding analyses. Cell *56*, 879-889.

Yang,J.T., Saxton,W.M., Stewart,R.J., Raff,E.C., and Goldstein,L.S. (1990). Evidence that the head of kinesin is sufficient for force generation and motility in vitro. Science *249*, 42-47.

Yang,Z., Roberts,E.A., and Goldstein,L.S. (2001). Functional analysis of mouse kinesin motor Kif3C. Mol. Cell Biol. *21*, 5306-5311.

Yu,H., Toyoshima,I., Steuer,E.R., and Sheetz,M.P. (1992). Kinesin and cytoplasmic dynein binding to brain microsomes. J. Biol. Chem. *267*, 20457-20464.

Zarsky,H.A., Cheng,M., and van der Hoorn,F.A. (2003). Novel RING finger protein OIP1 binds to conserved amino acid repeats in sperm tail protein ODF1. Biology of Reproduction *68*, 543-552.

Zou,Y., Millette,C.F., and Sperry,A.O. (2002). KRP3A and KRP3B: candidate motors in spermatid maturation in the seminiferous epithelium. Biol. Reprod. *66*, 843-855.